Investigating the relationships between remotely sensed and *in situ* drought indicators to understand streamflow discharge anomalies

by

Devon Ali Bandad

B.S., Kansas State University, 2017

A THESIS

submitted in partial fulfillment of the requirements for the degree

MASTER OF SCIENCE

Department of Biological & Agricultural Engineering
Carl R. Ice College of Engineering

KANSAS STATE UNIVERSITY
Manhattan, Kansas

2020

Approved by:

Major Professor
Vahid Rahmani

Copyright

Abstract

Predicting drought and streamflow are important aspects of water management to help mitigate the effects that a drought has on the environment and the people involved. The goals of this research are to assess remote sensing indicators and their ability to monitor drought and streamflow changes compared to *in situ* indicators in order to better estimate streamflow changes in times of drought in areas and at times without station-based data. Using *in situ* drought indicators such as station-based Palmer Drought Severity Index (PDSI) and Standardized Precipitation Index (SPI) helps water managers identify drought severity based on various environmental factors measured on a regular basis using station-based data. Remote sensing indicators on the other hand use satellite inputs to monitor such trends as vegetation coverage at a higher spatial resolution than an *in situ* index would. Remote sensing information is more readily available than most observed environmental information across the globe.

The study region is located in central United States in the MINK (Missouri, Iowa, Nebraska, and Kansas) region. Data for the growing period (April-September) from 2003-2017 were used. The region varies greatly from east to west in both land cover and average precipitation amount (318 – 1397 mm per year) as the region becomes drier and changes from forests in the southeast to farmland and prairie in the west.

The first part of the study evaluated various drought indices and their relationships with streamflow. The *in situ* indices evaluated include SPI and PDSI, which were available on a monthly basis for each climate division in the MINK region. The remote sensing indices include the Vegetation Condition Index (VCI) and the Soil Moisture Condition Index (SMCI). Each index has different data inputs, such a precipitation (PDSI and SPI) and temperature (PDSI) for the *in situ* indices and vegetation greenness (VCI) and soil moisture (SMCI) for the remote

sensing indices. The indices were ultimately compared both spatially and temporally (annual basis) to streamflow in the form of discharge anomalies (PDA).

In the second part of this study, analysis focused on how relationships between the remote sensing indices changed as land cover varies over the MINK region. Overall, results suggest that the *in situ* indices (PDSI and SPI) can estimate PDA changes (on an annual scale), while SMCI performed better than VCI overall though not as well as PDSI or SPI. The findings from this study have the potential to assist water managers and policy makers to better understand streamflow changes and increase drought preparedness.

Table of Contents

List of Figures

List of Tables

Acknowledgements

Firstly, I would like to thank my family and friends for supporting me through all the highs and lows over the years. Without their constant love and support I would not be where I am today. Secondly, I would like to thank my major professor Vahid Rahmani and committee members John Harrington Jr. and Andres Patrignani for their guidance and support throughout the research and writing of this work. I would also like to thank the USDA National Institute of Food and Agriculture, Hatch project KS545 and K-State Research and Extension 13-300-A for funding this research.

Dedication

I would like to dedicate this thesis to my mother and father. Both of which raised me to have a passion for what I believe in and a work ethic to chase my dreams, the journey is just getting started. I love you both more than you will ever know.

Chapter 1 - General Introduction

Droughts are one of the most widely spread and damaging natural hazards impacting agricultural environments and the people and the economy that depend on them. Since humans have begun to modernize, we have found solutions to many of the issues surrounding agriculture like insects, but drought has continued to decimate food supply and water resources (Palmer, 1965). During a drought, pressure is put on agriculture, water resources (including hydropower generation), human and animal health, which puts them in jeopardy (Svoboda & Fuchs, 2016).

Depending on the areas affected and length of the event, three broadly classified different physical types of droughts can occur: meteorological, agricultural, and hydrological drought (Zargar, Sadiq, Naser, & Khan, 2011). One type of drought can lead to another depending on the length. For instance, lack of precipitation can lead to meteorological drought, decreased soil moisture from lack of precipitation can lead to agricultural drought, and low recharge from the soil to water bodies like lakes and streams can lead to hydrological drought (Zargar, Sadiq, Naser, & Khan, 2011). If a drought lasts long enough, the negative effects on people and economic growth increase, which is termed socio-economic drought (Heim Jr., 2002). Droughts usually have a slow onset, which makes them able to be monitored by keeping track of the various contributors to drought including increased temperatures and below normal precipitation totals (Svoboda & Fuchs, 2016). Though droughts usually take time to have negative effects, the newer term flash droughts (such as the 2012 event in the central United States), have little rainfall and high temperatures that lead to quick decreases in soil moisture (Otkin, *et al.*, 2016).

For the past half century, researchers have been developing indices to characterize drought and help monitor different types of drought and climatic factors such as temperature and precipitation changes. The goal of these indices include the development of early warning

systems by using readily available data such as air temperature and precipitation, which can be used to track and reveal information relating to trends of climate and hydrologic conditions (Svoboda & Fuchs, 2016). With the ability to monitor and predict the onset of drought, water managers and policy makers for the areas affected can take steps to limit the damage droughts can have on the environment and people. The earlier drought indices developed used *in situ* (station-based) data, usually climate related (precipitation and temperature) at selected weather stations scattered throughout a region of interest.

The Palmer Drought Severity Index (PDSI) was one of the first meteorological drought indicators developed based on temperature and precipitation shortages (Palmer, 1965). Palmer developed the index in order to be independent of space of time (universal across the globe) that could be used for extended drought periods (Palmer, 1965). PDSI is calculated based on empirical equations that synthesize historical temperature and precipitation data into a simple drought indicator (Alley, 1984). The final output gives a numerical value for a single month representing wet or dry conditions for the place or region of interest with normal conditions being the median values on the PDSI scale. The National Oceanic and Atmospheric Administration (NOAA) has determined monthly PDSI values on a climate division scale for the United States dating back to 1895 (Karl, 1986). There are several strengths and weaknesses associated with using the PDSI. One major strength is that it has been widely adopted throughout the world for drought monitoring (Svoboda & Fuchs, 2016). Weaknesses of the indicator include the complexity of the equations to derive values and arbitrary rules to quantify the beginning and ending of drought (Alley, 1984).

Many other drought indicators have been developed to monitor different aspects of drought or specialize in different climates regimes (Heim Jr., 2002). One such indicator is the

Standardized Precipitation Index (SPI), which was developed in 1993 to quantify precipitation deficits or surplus compared to the long-term normal (McKee, Doesken, & Kleist, 1993). To calculate SPI, only monthly precipitation data is needed with averaging periods of varying time scales (1, 2, 3, 6, 9, 12, 24, and 48 months). SPI values with time periods in the lower range (less than 6 months) fluctuate more often than SPI values for time periods above 6 months (McKee, Doesken, & Kleist, 1993). Values that are positive represent greater than median precipitation while values below zero represent below median precipitation for that time period (Guttman, 1998). As with PDSI, the SPI index also has strengths and weaknesses that come with using it. Some strengths include: SPI is very simple to use since it only requires monthly precipitation data, it has varying time-scales to monitor different types of drought (agricultural and hydrological), and SPI is normalized to represent both wet and dry conditions similarly (Zargar, Sadiq, Naser, & Khan, 2011). On the other hand, one major weakness is also its greatest strength: using only precipitation data to monitor drought means cutting out the temperature component, which is important for calculating the water balance in a given region (Svoboda & Fuchs, 2016).

As satellite technology advanced throughout the late 20th century, remote environmental sensors have been widely used to monitor the Earth's surface. Remote sensing data, allows users to access large amounts of data that cover the entire Earth or a selected study region on a per pixel (picture element) basis. Depending on the sensor, the individual pixels can be as large as several kilometers or smaller than 30 meters in width. One of the first remote sensing indicators, the Normalized Difference Vegetation Index (NDVI), is used to monitor vegetation health using reflectance in the red and near infrared wavelengths (Tarpley, Schneider, & Money, 1984; Tucker, 1979). Countless other remote sensing drought indicators have been developed using

different satellite sensors and combining data from the sensing of different spectral bands to create more complex indicators. The Vegetation Condition Index (VCI) was developed using NDVI values to better monitor drought conditions (Kogan, 1990). Other indices monitor different aspects of the environment. For example, the Evaporative Stress Index (ESI) was developed to monitor drought using remotely sensed potential evapotranspiration (Anderson, Hain, Wardlow, Pimstein, & Mecikalski, 2011) or the Temperature Condition Index (TCI), Precipitation Condition Index (PCI), and Soil Moisture Condition Index (SMCI) all use similar input formulas with different datasets (remotely sensed temperature, precipitation, and soil moisture data respectively) (Zhang & Jia, 2013).

Remote sensing indicators are frequently tested for effectiveness in monitoring drought compared to well-known *in situ* indicators (like PDSI and SPI) that have been shown to monitor various aspects (duration and severity) of drought well. One such study was conducted in 2017 for the continental United States, which compared numerous remote sensing indicators including VCI and SMCI to PDSI and SPI for the drought events of 2011 into 2012 (Zhang, Jiao, Zhang, Huang, & Tong, 2017). The study showed areas in the Continental United States (CONUS) where VCI correlated well with PDSI and SPI on a climate division scale for the drought event. Another study looked at how well VCI can monitor drought on a county basis in Texas. The authors found that VCI correlated best with PDSI, SPI-6, and SPI-9 in the western half of the state (Quiring & Ganesh, 2010). VCI has shown to have stronger correlations with longer term drought indices such as PDSI and longer SPI time-scales (Jiao, *et al.*, 2016). VCI performs best compared to station-based data in the southern and southwest United States, primarily the semi-arid regions of the country (Zhang, Jiao, Zhang, Huang, & Tong, 2017).

SMCI showed the highest correlation with SPI-1 (short-term drought) in southwest China (Hao, Zhang, & Yao, 2015). This finding agrees with other studies that analyzed SPI. Another study in southwest China showed that SMCI had the highest correlation with SPI-3, which backs the finding that SMCI performs better at detecting short-term drought (Li, He, Quan, Liao, & Bai, 2015). The study also showed that the correlations between VCI and SPI were lower than those of SMCI-SPI, which might suggest vegetation growth is less responsive to precipitation variation in moist areas (Li, He, Quan, Liao, & Bai, 2015). Overall SMCI is best for monitoring short-term drought over large areas (Zhang, Jiao, Zhang, Huang, & Tong, 2017).

Water is one of the most important natural resources that is used for everything from drinking water and food production to navigation and recreational purposes, which makes drought monitoring an important aspect of water management. With the ever-growing human population, the demand for water is also ever growing due to its need for food production and human health (Rahmani, Hutchinson, Harrington Jr, Hutchinson, & Anandhi, 2015). Streams and rivers are a major source of freshwater that have allowed human civilizations to develop over thousands of years (Rahmani, *et al.*, 2018; Zhao, *et al.*, 2014). Due to their importance, stream gauge stations have been installed by various governmental agencies to monitor discharge changes among other streamflow characteristics. The effects of climate and land use changes on streamflow have shown that climate impacts are much higher than that of land use (Liu, *et al.*, 2013).

Predicting streamflow changes when discharge measurement stations are not available is an important aspect of water management (Haslinger, Koffler, Schoner, & Laaha, 2014). Knowing when a streamflow (hydrological) drought could occur would provide important information for managing water resources (Zhao, *et al.*, 2014). One way to accomplish this could

be to use drought indicators to predict streamflow changes. Studies have analyzed *in situ* indicators like PDSI and SPI to find the relationship that these indicators have with streamflow (Zhai, *et al.*, 2010). PDSI and SPI showed relatively high correlations with streamflow discharge anomalies, meaning that the indicators could be used to indicate streamflow variation (Zhai, *et al.*, 2010). Other studies have shown that there is a significant link between streamflow and meteorological drought using PDSI and SPI indicators (Haslinger, Koffler, Schoner, & Laaha, 2014). Since meteorological drought indices typically use station-based data, using remotely sensed drought indices to monitor streamflow changes would provide many advantages in areas that cannot afford the cost of station-based data. One of the main objectives of this work is to compare capabilities of remote sensing-based to station-based indicators for predicting streamflow anomalies.

If remote sensing drought indices could significantly predict streamflow changes like *in situ* indices have shown, then streamflow could be estimated during drought periods in areas or times without regular access to station-based data. This brings up the main question of this thesis: can remote sensing drought indices estimate streamflow (Percentage of Discharge Anomalies (PDA)) changes as effectively as *in situ* drought indices in the Missouri, Iowa, Nebraska, and Kansas (MINK) region? To answer this question four sub-questions need to be addressed: 1) how do the remote sensing (VCI and SMCI) indices compare to *in situ* indices (PDSI and SPI); 2) how do drought indices (PDSI, SPI, VCI, and SMCI) compare to PDA; 3) does the variability of drought indices (PDSI, SPI, VCI, and SMCI) follow the variability of PDA; and 4) how does land cover influence the remote sensing drought indices?

First, chapter 2 of this thesis discusses two remote sensing indices (VCI and SMCI) and compares them to two *in situ* indices (PDSI and SPI) for the MINK region. Second, the chapter

investigates streamflow Percentage of Discharge Anomalies (PDA) and examines the PDA relationship to each drought index. Chapter 3 of this thesis analyzes the effect land cover within the different parts of the study area has on the results from Chapter 2.

With this work, it is hoped that water managers and policy makers will use the results in order to better understand the relationship between drought indices and streamflow. If the results for the MINK region are promising, then perhaps the same indicators could be used in other regions to monitor drought and streamflow changes. With a better knowledge of the relationship between drought indices and streamflow, remote sensing estimates of streamflow could help mitigate the damages drought might have on the environment and people being affected.

Chapter 2 - Capability of remote sensing and *in situ* drought indices for assessing drought and streamflow

Introduction

Drought is one of the worst natural disasters that affects the environment (through plant degradation by water loss), humans, and the economy (by water, food, and crop loss) (Wen, Rogers, Ling, & Saintilan, 2011; Zhai, *et al.*, 2010). Monitoring drought is an important aspect of water management, with the goal of mitigating the effects a drought has on the environment and the people impacted. Droughts can cause major environmental degradation to areas with crop yield reduction from an agricultural drought perspective and loss of streamflow discharge from a hydrologic drought perspective. Many indicators have been developed over the past half century to help climatologists and meteorologists monitor the onset of drought and to help mitigate its effects (Zhang, Jiao, Zhang, Huang, & Tong, 2017). *In situ* drought indicators like the Palmer Drought Severity Index (PDSI) and the Standardized Precipitation Index (SPI) are typically computed using station-based climate data to monitor various components of droughts, like precipitation deficits and related temperature impacts (McKee, Doesken, & Kleist, 1993; Palmer, 1965).

Remote sensing data allow more efficient monitoring of changing surface conditions over wider areas at fine spatial resolutions (i.e. sub-kilometer scale) with easier measurability compared to *in situ* data (Tavakol, Rahmani, Quiring, & Kumar, 2019; Zhang, Jiao, Zhang, Huang, & Tong, 2017). Over the years, various remotely sensed drought indicators have been developed to monitor different aspects of drought (Quiring & Ganesh, 2010). The Normalized Difference Vegetation Index (NDVI), which is used to monitor vegetation health, was among the first vegetation-based indices developed to monitor greenness of the Earth's surface (Tarpley,

Schneider, & Money, 1984). The Vegetation Condition Index (VCI) is a drought index derived from NDVI and used to monitor the onset of droughts (Kogan, 1990). Another remote sensing environmental indicator is the Soil Moisture Condition Index (SMCI), which uses remotely sensed soil moisture for tracking short-term drought conditions over larger regions (Zhang & Jia, 2013; Zhang, Jiao, Zhang, Huang, & Tong, 2017).

The motivation for this work is to assess the value of using remote sensing indices to estimate streamflow changes during drought periods in order to be better prepared to mitigate the problems that arise from such an event. An important aspect of water management is to be able to predict streamflow changes in the absence of discharge data (Haslinger, Koffler, Schoner, & Laaha, 2014). Water managers and government agencies could use these indicators early on to help mitigate the potential negative effects of drought events on vulnerable environments and communities.

Methods and Materials

Study Area

The Great Plains and Middle West of the United States are home to vast agricultural lands where water resources are of great importance for crop yields, food security, and economic growth. The states of Missouri, Iowa, Nebraska, and Kansas (the MINK region) utilize both surface and ground water for irrigating croplands planted with corn, soybeans, and sorghum (Easterling, et al., 1993). Missouri and Iowa have many streams that have sustained flow throughout the year whereas western Kansas and Nebraska have little surface water for much of the year (Frederick, 1993; Rahmani, Hutchinson, Harrington Jr, Hutchinson, & Anandhi, 2015). The region varies from east to west in land cover and precipitation amounts (Fig. 2-1). Land cover data was used from the National Land Cover Database 2011 and annual precipitation data

was used from the PRISM Climate Group. The main land covers by percentage of area over the region are deciduous forest (11%), pasture and hay (13%), grassland and herbaceous (26%), and cultivated cropland (40%). The southeast portion of Missouri is primarily deciduous forest with a relatively high average annual precipitation (1397 mm) while the western part of the study region is semi-arid rangeland and irrigated cropland with lower average precipitation (318 mm). Average summer (July) high temperatures in the region are highest in Kansas with a temperature of 25 ℃ and lowest in Iowa at around 22.0 ℃ between 1981 and 2010 (NOAA, 2019).

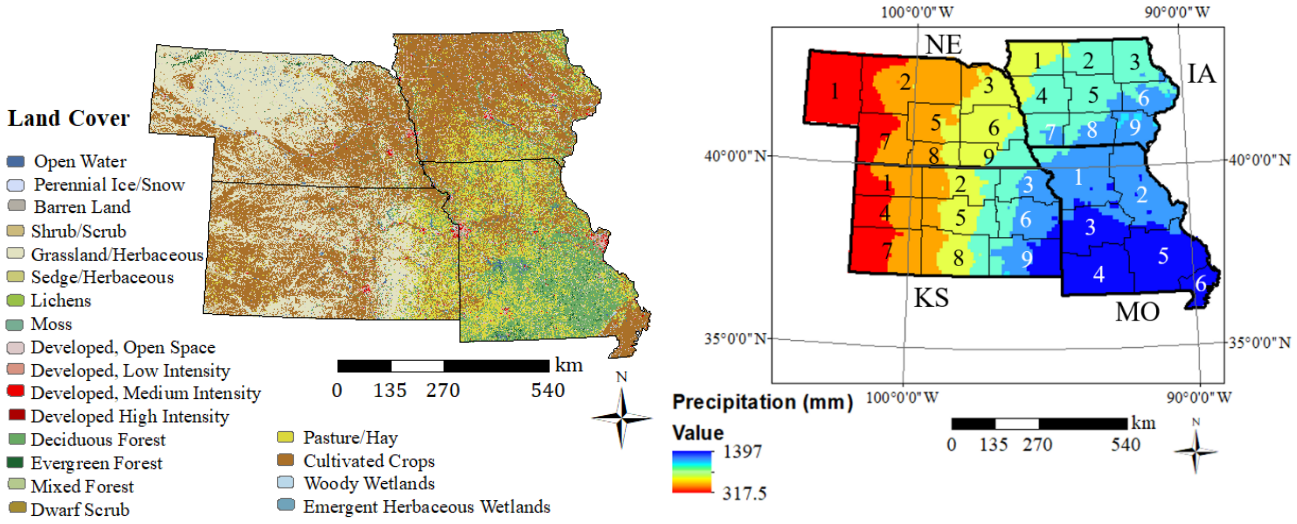

Figure 2-1. Maps of United States showing location of the MINK region with climate divisions, land cover, and total annual precipitation variation.

Methods

For this study, several *in situ* and remotely sensed datasets were used for calculating each environmental indicator. To observe recent relationships in the Missouri, Iowa, Nebraska, and Kansas (MINK) region, data from 2003 through 2017 over the growing season of April through September on a monthly basis was used for the study. The growing season is the focus because it is the time period when droughts have more severe impacts, especially on crop growth.

In Situ Drought Indices

The two *in situ* (station-based) drought indices used in this study are PDSI and SPI, both of which have been widely used for evaluating the effectiveness of remote sensing indicators in monitoring various aspects of drought. The PDSI has been widely used for many decades to monitor droughts in the United States. This meteorological index uses station measured precipitation, temperature, and soil water budget to estimate the available water content of the soil (Palmer, 1965). The soil water budgeting requires evapotranspiration, potential evapotranspiration, soil water recharge, potential recharge of the soil, runoff, potential runoff, water loss from soil, potential water loss from the soil, and precipitation data (Karl, 1986). PDSI values generally range from -10 to +10. A value lower than -4 is considered extreme drought while a value greater than +4 is considered extreme wet conditions. Values between -1 to +1 are considered normal. Deriving monthly PDSI is outlined in greater detail in Karl (1986). The monthly PDSI equation is shown below where $PDSI_i$ is monthly PDSI, $PDSI_{i-1}$ is the previous monthly PDSI value, and Z_i is the moisture anomaly index for the specific month:

$$PDSI_i = PDSI_{i-1} + \frac{1}{3}Z_i - 0.103PDSI_{i-1} \quad (1)$$

The SPI is based on quantifying precipitation as a deficit or a surplus compared to the long-term normal (McKee, Doesken, & Kleist, 1993). SPI values lower than -2.0 are classified as extreme drought while values greater than +2.0 are considered extremely wet conditions. SPI also classifies values below -1.0 as dry, above +1.0 as wet, and between -1.0 to 1.0 as near normal (Zhai, et al., 2010). SPI can be computed for time period ranges of 1, 2, 3, 6, 9, 12, and 24 months (SPI-1 to SPI-24). When time periods are short (less than 6 months), SPI moves frequently above and below zero. As the time period increases, SPI responds more slowly to changes in environmental conditions (McKee, Doesken, & Kleist, 1993). The equation for SPI is

shown below, where P is precipitation, P^* is mean precipitation, and σ_p is the standard deviation of precipitation.

$$SPI = (P - P^*)/\sigma_p \quad (2)$$

In Situ Drought Index Data

Monthly values of PDSI and SPI were obtained from the NOAA National Centers for Environmental Information (NCEI) (https://www.ncdc.noaa.gov/) on a climate division scale for the region. The data is derived from stations across each climate division using area-weighted averages of estimates interpolated from the stations (Vose, et al., 2014). In this study, monthly drought indicator values are directly compared to the derived remotely sensed indicators and PDA values for the growing season months from 2003 to 2017.

Remote Sensing Indices

The VCI is derived directly from the NDVI. NDVI is one of the oldest remote sensing indices and is relatively simple in its approach for assessing vegetation health based on infrared and visible bands from satellite data (Kogan, 1990). Vegetation greenness is estimated on a per pixel basis using the difference in reflectance between visible (red) light and near-infrared (NIR) light:

$$NDVI = \frac{VISIBLE - NIR}{VISBLE + NIR} \quad (3)$$

NDVI values range from -1 to +1 with values near 0 having little to no green vegetation and values near +1 having full green vegetation density (Tarpley et. al., 1984; Quiring and Ganesh, 2010). Compared to NDVI, VCI is better for estimating drought intensity because it incorporates various weather impacts such as precipitation changes on vegetation (Kogan, 1990). VCI for each month is determined as:

$$VCI_i = \frac{NDVI_i - NDVI_{min}}{NDVI_{max} - NDVI_{min}} \quad (4)$$

Where $NDVI_i$ is the NDVI value for a given month, and $NDVI_{min}$ and $NDVI_{max}$ are the absolute minimum and maximum values for the entire NDVI record (2003-2017 in this study). VCI values range from 0 to 1, where values near 0 suggest little vegetation and 1 suggests a pixel fully covered with vegetation.

SMCI is an index solely derived from remotely sensed soil moisture data that estimates soil moisture in kilogram per square meter for the top 10 centimeters of soil surface. The index values range from 0 to 1 with 0 indicating extreme drought and 0.5 to 1 showing no drought (Zhang & Jia, 2013; Zhang, Jiao, Zhang, Huang, & Tong, 2017). SMCI for each month is estimated as:

$$SMCI_i = \frac{SM_i - SM_{min}}{SM_{max} - SM_{min}} \quad (5)$$

Where SM_i is the average soil moisture for a given month, SM_{min} and SM_{max} are the absolute minimum and maximum values for soil moisture over the entire record from 2003 to 2017.

Remote Sensing Drought Index Data

Moderate Resolution Imaging Spectroradiometer (MODIS) 250 meter resolution NDVI values were used from the NASA Earth data center (https://search.earthdata.nasa.gov/) to derive VCI values on a per-pixel basis. All 250 meter pixels within a given climate division were used and the median value of all pixels was selected as the climate division value for a given month. NASA's North American Land Data Assimilation System (NLDAS-2) NOAH land-surface model composites (https://disc.gsfc.nasa.gov/datasets?keywords=NLDAS) for remotely sensed soil moisture was used to calculate SMCI on a monthly basis. This data has a 1/8 degree (~13.875 km) resolution and the top 10 centimeter soil moisture depth was used for SMCI. The

mean of all SMCI pixel values within a climate division was used as a single climate division value.

Streamflow Percentage of Discharge Anomalies

PDA was used to compare monthly streamflow changes with each of the four drought indicators (Zhai, *et al.*, 2010). The following equation was used to calculate the PDA for each month:

$$\mathrm{PDA_i} = \frac{(\mathrm{X_i} - \overline{\mathrm{X}})}{\overline{\mathrm{X}}} \quad (6)$$

Where $\mathrm{X_i}$ is the average discharge for a given month, and $\overline{\mathrm{X}}$ is the average discharge (m^3/s) for the entire time period from 2003-2017 for a given month.

Streamflow Data

Discharge data were downloaded from the US Geological Survey (USGS) water services site for gauge station data (https://waterservices.usgs.gov/). Data for 117 stream gauges were available for the region (Fig. 2-2). For each climate division, two to four stream gauge stations were used with a mix of reference and non-reference conditions. Stations with reference conditions are those, whose flow has minimal impact from human and other anthropogenic activities and the site conditions may reflect natural changes like drought influences. Non-reference sites could have an array of various human influences like water discharge for human consumption or a dam upstream from the gauge station that would influence discharge through the gauge site. The watershed size for the selected stream gauges varied from 65.5 km^2 to 221,703 km^2. The Nebraska 1 climate division (i.e. the Nebraska Panhandle) had several years with 0 values for the one station in the region and it was excluded from the analysis.

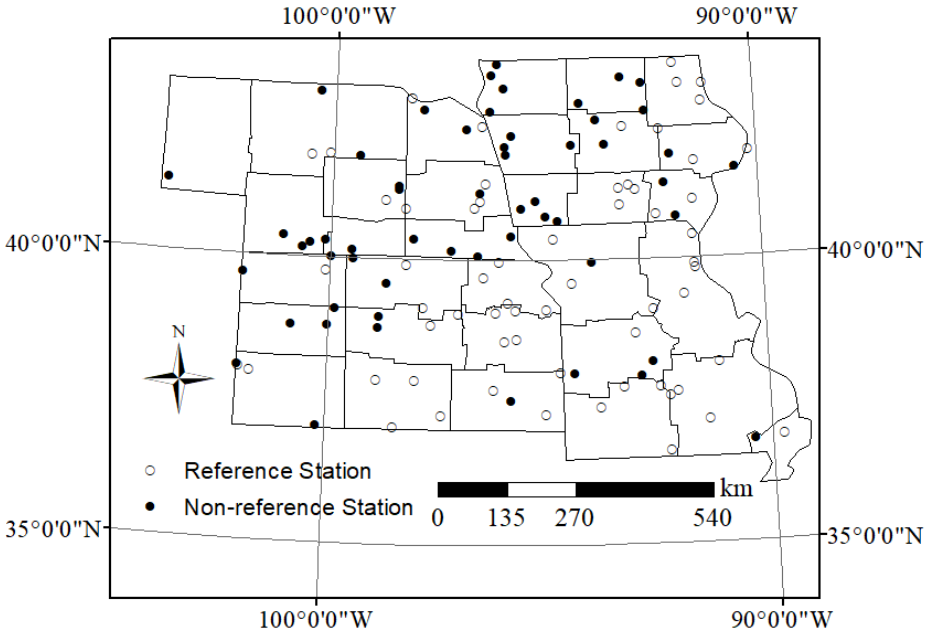

Figure 2-2 Climate division boundaries and location of all USGS stream gauges used in the study.

Results and Discussions

Comparing Remote Sensing to *In Situ* Drought Indices

Remote sensing indicators of VCI and SMCI were evaluated against the *in situ* indicators of PDSI and SPI. The Pearson correlation (r) and coefficient of determination (R^2) values were calculated for each relationship and division over the 15-year period (Fig. 2-3 and Table 2-1). Overall, SMCI performed better than VCI when correlated with the *in situ* indicators and performed better with short-time scale SPIs (1–3) than PDSI throughout the entire region. SMCI had a statistically significant relationship with PDSI, SPI-1, and SPI-3. SPI has been shown to correlate well with soil moisture, which is the basis for SMCI (Vicente-Serrano, et al., 2012). As the SPI time periods become longer than SPI-3, its relationship with SMCI generally becomes weaker. SMCI was shown to have its strongest correlation with SPI-3 in a study conducted in China (Li, He, Quan, Liao, & Bai, 2015). Since SMCI is based on soil moisture, it is more highly influenced by the climatic factors of precipitation and temperature compared with VCI, which

can be influenced by a variety of non-climatic factors such as plant disease, insects, and human influences such as land use changes. As a result, SMCI has higher correlations with the *in situ* indices over the region than VCI. This conclusion suggests SMCI is more susceptible to climatic factors that influence both PDSI and SPI (i.e. precipitation and temperature) than VCI.

VCI performed best with SPI-2 but also was fairly strongly correlated with most other SPI time series indices in the western part of the region. VCI had stronger correlations with PDSI and SPI in Kansas and Nebraska (Table 2-1) which, is similar to the findings from Zhang, Jiao, Zhang, Huang, & Tong (2017). Quiring & Ganesh (2010) found that VCI performed better with PDSI and SPI in western (drier) parts of Texas than in the eastern (wetter) part. Drier climates have different vegetation types (perhaps with more bare soil), so during a drought event, VCI will not have the same response in both types of climate. VCI could have higher correlations in drier regions partially due to vegetation types (shallow rooted-grasses) that are more effected by varying climate conditions compared to vegetation types (longer rooted-grasses and trees) with wetter conditions. VCI had lower correlations with the *in situ* indicators in irrigated land due to irrigation having a positive effect on vegetation health (VCI) that has no effect on meteorological indices like PDSI and SPI (Quiring & Ganesh, 2010). The most heavily irrigated part of the MINK region is eastern Nebraska (Irrigation & Water Use, 2019), which had weaker correlations between VCI and the *in situ* indicators. Analyzing the irrigated land relationships at smaller scales than the scope of this study (climate division rather than state level) would provide more information on the performance of VCI.

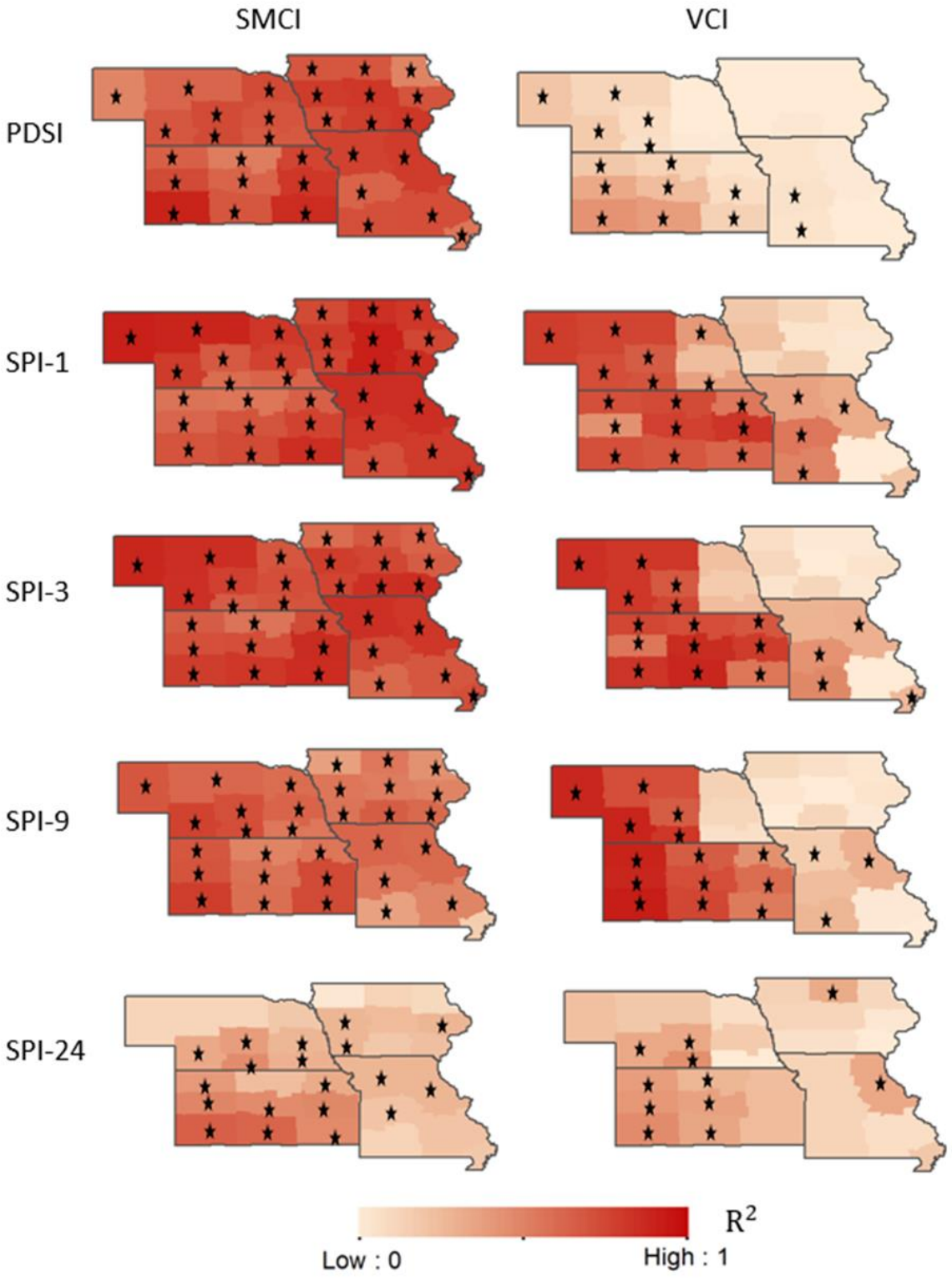

Figure 2-3 R^2 values for temporal correlation (yearly) from 2003 to 2017 between corresponding drought indices in the MINK region. Stars indicate climate divisions with a statistically significant correlation with $\alpha = 0.05$.

Analysis of the correlations based on data summarized for each state indicate the highest correlations between VCI and PDSI in Kansas followed by Nebraska, Missouri, and Iowa (Fig. 2-3 and Table 2-1) (Bandad & Rahmani, Analysis of PDSI and Vegetation Condition Index (VCI) and Their Links to Streamflow, 2018). SMCI performed better in all four states for PDSI and SPI-1–3. The performance was weaker for SPI-6–24 with higher correlations in Kansas and Nebraska compared to Iowa and Missouri. SMCI estimates upper level soil moisture which is more highly influenced by short term changes, so a higher predictability (R^2) is expected with the shorter-time scale SPIs. Generally, SMCI performed better than VCI indicating SMCI is more influenced by climatic factors like precipitation, which greatly influences streamflow. But when comparing state by state, VCI performs comparatively similar to SMCI in Kansas and Nebraska, where VCI has its best performance.

Table 2-1 Average R^2 values comparing the *in situ* and remote sensing drought indicators for the MINK region and each state.

	MINK Region		Kansas		Nebraska		Iowa		Missouri	
	SMCI	VCI	SMCI	VCI	SMCI	VCI	SMCI	VCI	SMCI	VCI
PDSI	0.71	0.41	0.73	0.68	0.68	0.51	0.73	0.11	0.70	0.30
SPI-1	0.77	0.43	0.69	0.68	0.76	0.58	0.82	0.11	0.81	0.33
SPI-2	0.78	0.45	0.75	0.73	0.79	0.60	0.79	0.09	0.78	0.38
SPI-3	0.75	0.42	0.75	0.74	0.77	0.57	0.73	0.04	0.74	0.29
SPI-6	0.54	0.33	0.63	0.66	0.57	0.46	0.44	0.01	0.53	0.16
SPI-9	0.59	0.38	0.66	0.71	0.66	0.53	0.53	0.04	0.47	0.16
SPI-12	0.55	0.37	0.64	0.65	0.58	0.48	0.54	0.09	0.42	0.23
SPI-24	0.29	0.21	0.46	0.33	0.27	0.22	0.19	0.10	0.21	0.16

Comparing the Drought Indices to PDA

Coefficient of determination (R^2) values were averaged for the relationships between each drought index and PDA for the MINK region and each state individually (Table 2-2). For R^2 values for each individual watershed and statistically significant relationships (shown by bolded values), please see appendix A. Generally, it is expected that changes at reference stream gauges have stronger correlations with natural phenomena such as droughts (Lorenzo-Lacruz, et

al., 2010). Building reservoirs on streams mitigates the effect that wet and dry seasons can have on a river system (Wen, Rogers, Ling, & Saintilan, 2011): the proportion of runoff during the rainy season decreases while the proportion of runoff during the dry season increases due to regulation (Ren, Wang, Li, & Zhang, 2002; Wen, Rogers, Ling, & Saintilan, 2011). In order to investigate this idea, stream gauges were separated into reference and non-reference sites. Relationships between drought indicators and PDA had slightly higher R^2 values for reference sites except for SPI-24 (Table 2-2) suggesting that the indices can predict streamflow better for reference watersheds. Generally, SPI-3 (R^2 = 0.49) and PDSI (R^2 = 0.48) indicated stronger predictability for PDA in the region. SMCI performed better than VCI when analyzed against PDA. SMCI and PDA are influenced by soil moisture and climatic conditions (such as changes in precipitation) more than VCI resulting in stronger relationships between SMCI and PDA.

Most indices had comparatively higher R^2 with PDA in Iowa except VCI and SPI-24 (Table 2-2 and Fig. 2-4). PDSI correlations produced similar R^2 values in Iowa and Nebraska. VCI had a stronger relationship with PDA in Kansas and Nebraska where VCI performs better in predicting drought (Bandad & Rahmani, 2019). SPI-24 correlations with PDA were also stronger in Kansas and Nebraska than the other two states. SMCI and PDSI performed comparatively well with PDA compared throughout the region but PDSI performed better overall.

Table 2-2 Overall average R^2 values for correlations between PDA and each drought index for each state in the region and separated into reference and non-reference gauge stations.

	MINK Region			Kansas			Nebraska			Iowa			Missouri		
	All	Ref	Non-Ref	All	Ref	Non-Ref	All	Ref	Non-Ref	All	Ref	Non-Ref	All	Ref	Non-Ref
SMCI	0.38	0.39	0.37	0.34	0.36	0.30	0.35	0.34	0.36	0.46	0.49	0.45	0.31	0.34	0.24
VCI	0.19	0.21	0.17	0.32	0.35	0.27	0.24	0.25	0.24	0.05	0.02	0.06	0.15	0.16	0.13
PDSI	0.48	0.50	0.47	0.46	0.44	0.49	0.53	0.58	0.52	0.52	0.60	0.47	0.42	0.47	0.33
SPI-1	0.43	0.46	0.39	0.31	0.37	0.22	0.39	0.37	0.40	0.54	0.61	0.51	0.44	0.48	0.34
SPI-2	0.46	0.51	0.41	0.36	0.42	0.25	0.41	0.40	0.41	0.56	0.66	0.51	0.48	0.53	0.38
SPI-3	0.49	0.54	0.44	0.40	0.47	0.29	0.44	0.43	0.45	0.58	0.68	0.52	0.52	0.56	0.44
SPI-6	0.44	0.51	0.39	0.40	0.45	0.32	0.36	0.34	0.37	0.50	0.66	0.41	0.50	0.53	0.45
SPI-9	0.46	0.51	0.42	0.41	0.45	0.34	0.43	0.45	0.43	0.53	0.65	0.46	0.45	0.48	0.39
SPI-12	0.41	0.42	0.39	0.39	0.40	0.37	0.45	0.50	0.44	0.46	0.52	0.43	0.31	0.35	0.23
SPI-24	0.24	0.22	0.26	0.31	0.27	0.39	0.31	0.36	0.30	0.20	0.22	0.19	0.10	0.10	0.11

The spatial pattern of PDA predictability for each drought indicator is presented in Figure 2.4 for all 117 individual gauge streams. The MINK regional average of R^2 was 0.48 for PDSI-PDA with a slightly weaker relationship in the southern states of Missouri (R^2 = 0.42) and Kansas (R^2 = 0.46) and stronger relationships in the northern states of Nebraska (R^2 = 0.53) and Iowa (R^2 = 0.52). SPI performs best in predicting PDA in Iowa with an average R^2 = 0.58 for SPI-3. Iowa includes the highest density of larger R^2 values for most SPI durations (Figure 2-4). The higher statewide average R^2 values for Iowa could be due to the higher number of reference stations, where relationships are generally stronger. VCI correlations with PDA produced the weakest average R^2 values in Nebraska (R^2 = 0.24) and Iowa (R^2 = 0.05) compared to the other three indicators. SPI-24 correlations with PDA produced the weakest R^2 values for Missouri (R^2 = 0.10) and SPI-1 and SPI-24 for Kansas (R^2 = 0.31). Quiring & Ganesh (2010) and Zhang, Jiao, Zhang, Huang, & Tong (2017) also found that VCI has higher correlations with PDSI and SPI in semi-arid regions, which suggests that VCI is better for monitoring PDA in the western part of the study region. SMCI correlations with PDA generates relatively strong R^2 values throughout the region with Iowa showing the highest density of higher values (R^2 = 0.46).

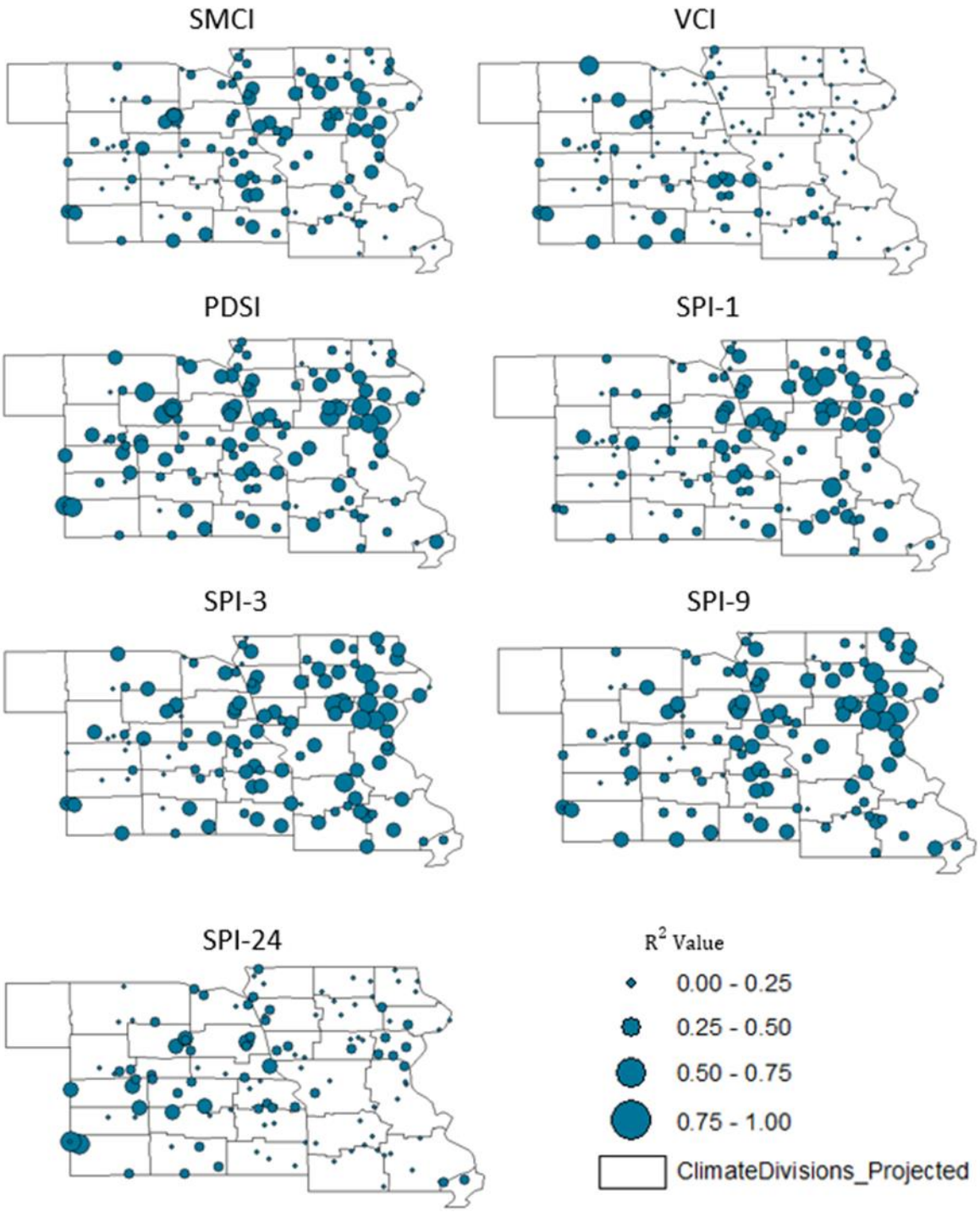

Figure 2-4 Maps showing the coefficient of determination (R^2) of temporal correlation between PDA and the corresponding drought indicators at each stream gauge.

Figure 2-5 indicates that Pearson correlation (r) values were strongest for intermediate values of SPI (e.g., SPI-3) and slightly weaker for shorter and longer SPI indices. Guttman (1998) found that longer time scales of SPI are better for addressing water supply changes

(hydrologic drought) rather than short term shifts (meteorological or agricultural drought), which lead to longer SPI values having less predictability for most droughts. As the time scale of SPI becomes longer, the correlation difference between reference and non-reference stations in average R^2 value becomes less (Fig. 2-5). For SPI-24, non-reference stations have a higher average R^2 with PDA than reference stations. Lorenzo-Lacruz *et al.* (2010) analyzing reservoirs in Spain found higher correlations between the inflows into reservoirs and shorter-time scale SPI indices compared to the outflows. They concluded that lower correlations were due to dam operations limiting the natural flow of water through the basin. Similar to the findings of this study, longer SPI time-scales had higher R^2 (> 0.42 values with 25 month or greater SPI indices) in Lorenzo-Lacruz *et al.* (2010). When prolonged droughts occur, reservoir operation adapts to the low water availability and outflows from the reservoirs will be more stable.

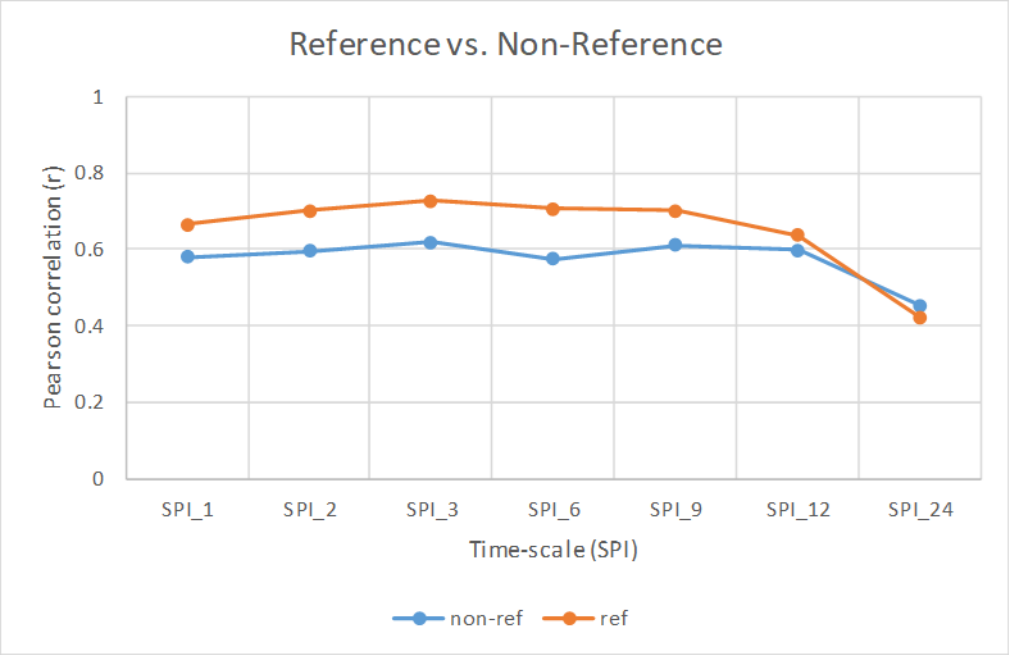

Figure 2-5 Average Pearson correlation (r) values for different timescale SPI indices and PDA for 117 river locations.

Yearly Variability Analysis between PDA and the Drought Indices

Figure 2-6 provides the annual values of each drought indicator and PDA for selected climate divisions over the 15-year study period (2003-2017). Six representative climate divisions are provided in the figure, with similar analyses completed for all climate divisions. The six selected climate divisions provide for a wide range of locations within the study region with the outer corners (NE 2, IA 3, MO 5, and KS 7) and the inner portion of NE 9 and KS 9. Only one PDA and SPI-1 are included in the figure to avoid clutter but other PDAs and SPI time scales had similar patterns. Overall, PDSI and SPI-1 yearly variability followed PDA variability for each division better than VCI and SMCI. A good example of this can be seen in 2012 where extreme drought covers most of the region. This finding suggests that PDSI and SPI can be used to estimate discharge anomalies during droughts and agrees with other studies on the effectiveness of meteorological indices for monitoring streamflow (Zhai, *et al.*, 2010; Zhao, *et al.*, 2014). Ahiablame *et al.* (2017) analyzed the relationship between precipitation and baseflow for the Missouri River Basin covering all of Nebraska and large portions of Kansas, Missouri, and Iowa. The study showed that precipitation and river discharge were closely related for a majority of gauge stations evaluated. Due to the strong relationship between discharge and precipitation, it can be understood why PDSI and SPI-1 (which rely on precipitation data) have a similar year to year variability with PDA varying between high and low values.

SMCI also showed similar yearly variability with PDA across the region. For the 2011-2012 drought, SMCI values seemed to be at a 15-year low point across the region as PDA was also at a low point. Overall, SMCI showed more similar yearly variability with PDA than VCI. Just as in the other tests, SMCI performs better with PDA and the *in situ* indices than VCI due to soil moisture being highly influenced by similar factors (i.e. precipitation) directly rather than

vegetation greenness. VCI tends to have little year to year variability for most divisions, though drought events (like 2011-2012) do have some effect on VCI with the region showing lower values. This might be due to the annual cycles of vegetation growth and how long it takes land cover to change over time.

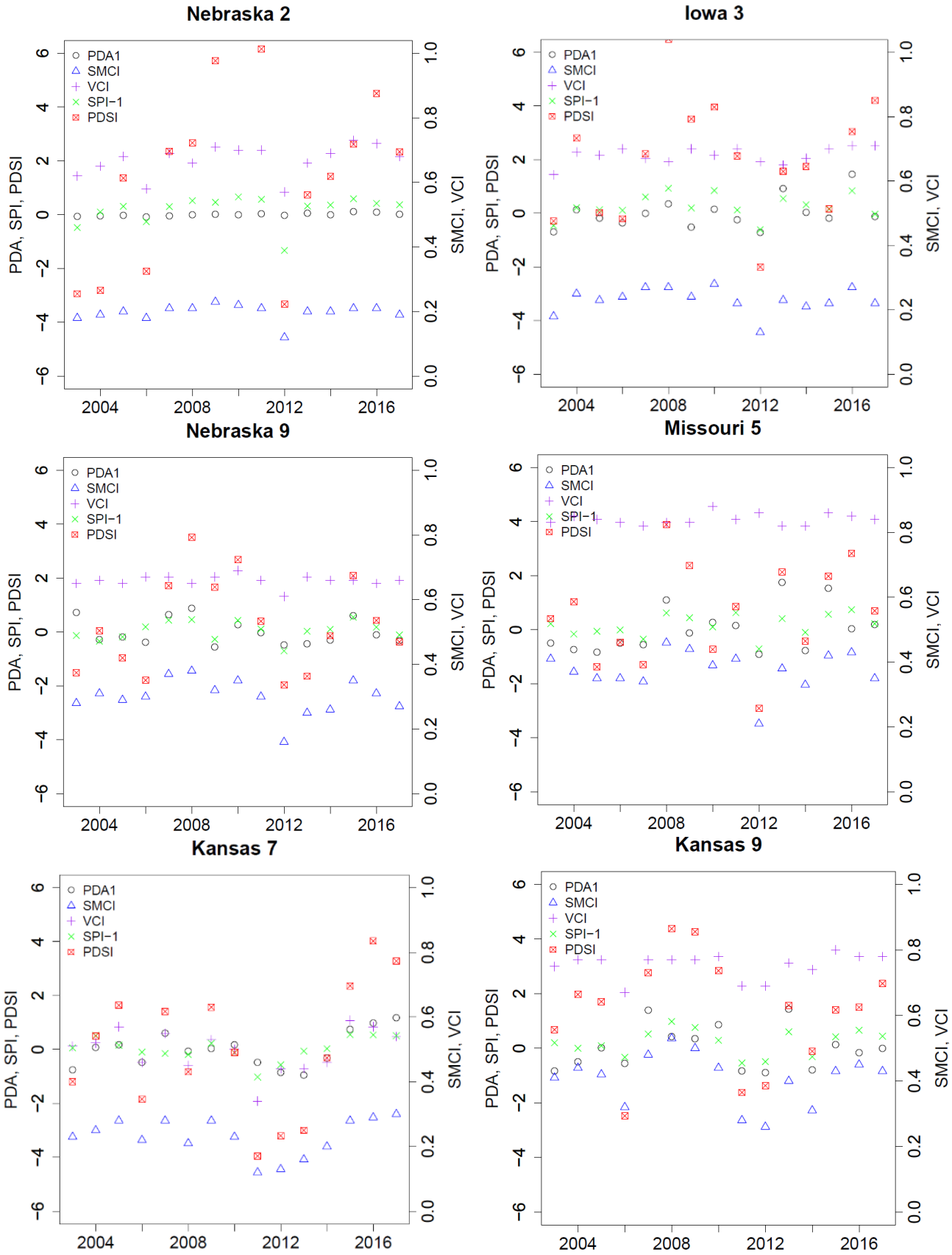

Figure 2-6 Graphs showing yearly variability of SPI-1, PDSI, VCI, SMCI, and PDA.

Summary and Conclusions

With easy access to large amounts of near real-time satellite data, remote sensing drought indicators may provide valuable information for drought monitoring over wide sections of land, like the U.S. Great Plains (AghaKouchak, *et al.*, 2015). This study evaluated two remote sensing indicators (VCI and SMCI) against two well-known *in situ* drought indicators (PDSI and SPI). Spatial and temporal changes of all indicators were analyzed to determine their performance in monitoring streamflow discharge anomalies (PDA) in the states of Missouri, Iowa, Nebraska, Kansas (the MINK region). Three methods for evaluating the effectiveness of the remote sensing indicators were discussed: 1) comparing the remote sensing indicators to the *in situ* indicators directly for each of 32 climate divisions, 2) comparing the drought indicators to PDA for each of 117 stream gauge stations within the region, and 3) assessing yearly variability from 2003 to 2017 for the various drought indicators and PDA.

In comparing the remote sensing indicators (VCI and SMCI), the results indicated stronger R^2 values for correlations between SMCI and both PDSI and SPI over the entire region with relationships for most climate divisions being statistically significant at $\alpha = 0.05$. SMCI estimates soil moisture, which is more influenced by climatic factors such as precipitation and temperature, whereas VCI addresses vegetation health. VCI tended to perform better in the western and more semi-arid regions of Kansas and Nebraska. Both *in situ* indicators (PDSI and SPI) performed better than the remote sensing-based indicators (SMCI and VCI) at predicting PDA.

Meteorological drought indices, such as PDSI and SPI, have shown good performance in monitoring streamflow changes especially during a drought (Zhai, *et al.*, 2010; Zhao, *et al.*, 2014). This is due to the fact that streamflow discharge is highly dependent on precipitation, soil

moisture, and temperature (not to mention human water use), which are the main inputs for both PDSI and SPI (Zhao, *et al.*, 2014). For estimating PDA, PDSI produced the highest R^2 values for the western states of Kansas and Nebraska while SPI-3 had the highest predictability power for the eastern states of Iowa and Missouri. SMCI had higher R^2 values with PDA than VCI in the region for most climate divisions (78%). Smaller scale analysis on irrigation and precipitation changes in the region could improve our understanding of this behavior of the SMCI.

This work indicated the potential of using near real-time satellite data and remote sensing indicators to monitor drought and changes in streamflow in the MINK region. Overall, SMCI performed better than VCI against *in situ* measurements and predicting PDA patterns. PDSI and SPI performed better at estimating PDA than both remote sensing indicators. Western semi-arid region of the MINK region is more appropriate for employing VCI. Water managers can use these remote sensing drought indicators for monitoring and predicting droughts when making decisions on how to use surface and groundwater, particularly during drought periods.

Chapter 3 - Evaluating the relationship between remote sensing drought indices and land cover

Introduction

Monitoring drought to mitigate the effects they have on the environment and people is one of the most important aspects of water management. Droughts can have severe detrimental effects on land cover (crop losses) and streamflow. To lessen the effects drought has on agriculture (crops and livestock) and water resources, it is important to be able to monitor the onset of drought by using drought indices (Svoboda & Fuchs, 2016). Remote sensing technology has allowed the development of drought indices for estimating vegetation and soil moisture over large areas (Zhang, Jiao, Zhang, Huang, & Tong, 2017). Being able to monitor drought gives water and land managers a tool to help prepare methods to limit the negative effects of drought. Since drought indices have begun to be evaluated, there have been differences in performance not just among indices but differences using the same indices for various locations or land cover (Quiring & Papakryiakou, 2003). One study showed that the relationship between VCI and SPI was strongest in dry-farming areas due to vegetation health being more effected by climatic factors when irrigation is not influencing natural trends (Vicente-Serrano, 2007). Another study evaluated human influences on NDVI in China and found that rapid urbanization has caused sharp decreases in NDVI, while in other areas NDVI has increased due to irrigation and fertilization (and increased plant growth) (Piao, *et al.*, 2003).

The goals of this study are to assess the impact of land cover on the relationships between each drought index and the relationships between the drought indices and PDA. For example, does land cover influence why VCI performs better in the western part of the Missouri, Iowa, Nebraska, Kansas (MINK) region while SMCI showed fairly high correlations with PDSI

and SPI throughout the region? Spatial patterns like these can influence the correlations between each drought index with PDA. As land cover varies throughout the study region from east to west, the region also becomes drier. The following analysis looks in depth at the relationships of each drought index with land cover by comparing VCI and SMCI to the main land cover types in the region by area (cultivated cropland, pasture and hay, grassland and herbaceous, and deciduous forest). Each land cover type is compared (through R^2 analysis) to VCI and SMCI on a climate division scale (larger area) and watershed scale (smaller area).

Methods and Materials

Study Area

The area of interest is a section of the Midwest United States coined the MINK (Missouri, Iowa, Nebraska, and Kansas) region. This area is part of the Great Plains, which has a huge agricultural economy focusing primarily on corn, wheat, soybeans, grain sorghum, and livestock such as cattle ranching (Easterling, *et al.*, 1993). Due to its role in crop production, water resource management is of great importance in the region, which primarily relies on streamflow and ground water supplies (Frederick, 1993). The region varies greatly in land cover and precipitation amounts when going from southeast Missouri to western Kansas and Nebraska. Figure 3-1a shows how the land cover in the region changes from primarily deciduous forest (green) in southern Missouri to cultivated cropland (brown) in Iowa and varying cropland and grassland (tan) in Kansas and Nebraska. These land cover changes are in part (along with temperature, topography, and soil types) due to the considerable variation in precipitation from east to west in the region with southeast Missouri averaging as much as 1,397 mm per year and western Kansas and Nebraska averaging as low as 317 mm (Fig. 3-1b).

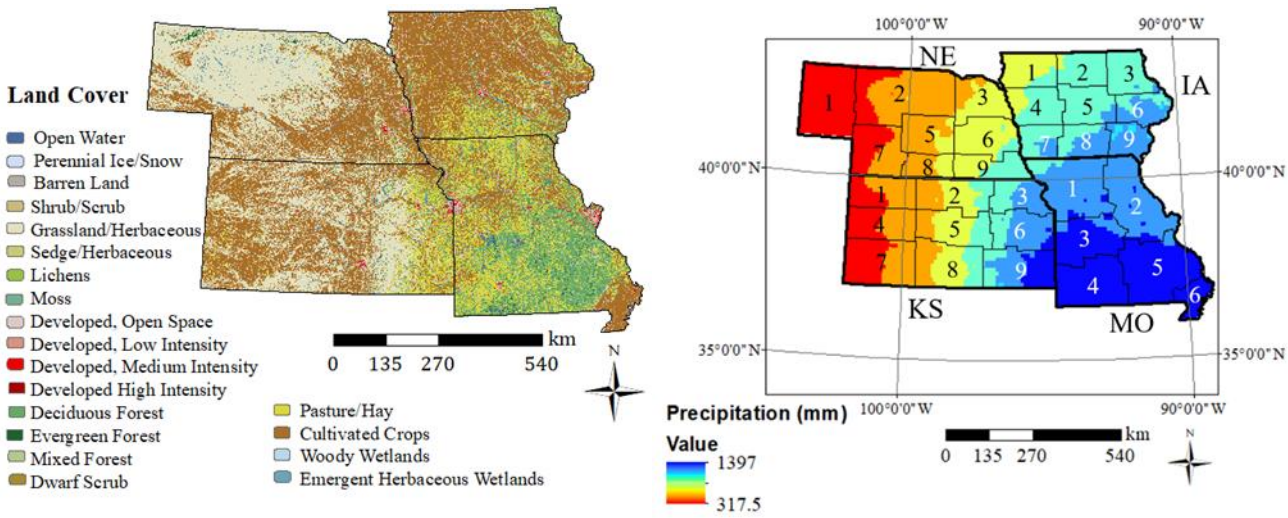

Figure 3-1 Maps of the MINK region with 1a) land cover and 1b) total annual precipitation variation with climate divisions.

Methods

Building on the analysis in chapter 2, which calculated each drought indicator (VCI, SMCI) on a climate division scale to be compared to the *in situ* indices (PDSI, SPI), this study focuses more so on the watersheds themselves. To do this, both VCI and SMCI index values needed to be determined for each specific watershed used. Using data for the growing season (April-September) from 2003 through 2017, both indicators were calculated on a watershed scale. The growing season was chosen due to the fact that droughts have a greater impact on crop growth during this time.

Remote Sensing Drought Indices

VCI is calculated directly from the NDVI, which is calculated using the difference between two spectral bands (Red and Near Infrared) to measure variations in the greenness of the Earth's surface on a per pixel basis (Kogan, 1990; Tarpley, Schneider, & Money, 1984). For more details on VCI and calculations, please refer to the methods section of chapter 2. For the climate division-based results the median of all VCI pixels within a climate division were used for calculations. Using the *modelbuilder* application in ArcGIS for watersheds in Kansas, Iowa,

and Missouri, the median value of all VCI pixels within a given watershed determined watershed scale VCI.

SMCI is calculated using remotely sensed soil moisture for the top 10 cm in a similar fashion as VCI (Zhang & Jia, 2013). For more details over calculating SMCI, please refer to the methods section of chapter 2. Chapter 2 uses average SMCI on a climate division basis for comparing to PDSI and SPI. For this analysis, average SMCI needed to be determined using *modelbuilder* in ArcGIS to derive watershed scale average values.

Data

Remote Sensing Drought Indices

VCI was calculated using MODIS 250 m resolution pixel NDVI values from NASA's Earth data site (https://search.earthdata.nasa.gov/).

SMCI was derived using the 13.875 km pixel resolution remotely sensed soil moisture for the top 10 cm into the surface. The data was acquired from NASA's North American Land Data Assimilation System (NLDAS-2) NOAH composites (https://disc.gsfc.nasa.gov/datasets?keywords=NLDAS).

Land Cover

Land cover data from the 2011 United States land cover shape file (National Land Cover Database 2011) was used at 30 m pixel resolution with each pixel representing the dominant land cover type at that location (refer to Figure 3-1 above).

Watersheds

Watersheds for each gauge station in the region except Nebraska (as Nebraska does not have StreamStats available) were delineated using USGS StreamStats (https://streamstats.usgs.gov/ss/) and downloaded to see the effects land cover in the basin area

has on the results of this study. Figure 3-2a below shows the location of USGS stream gauges and Figure 3-2b shows watershed sizes for each stream gauge (excluding gauges in Nebraska).

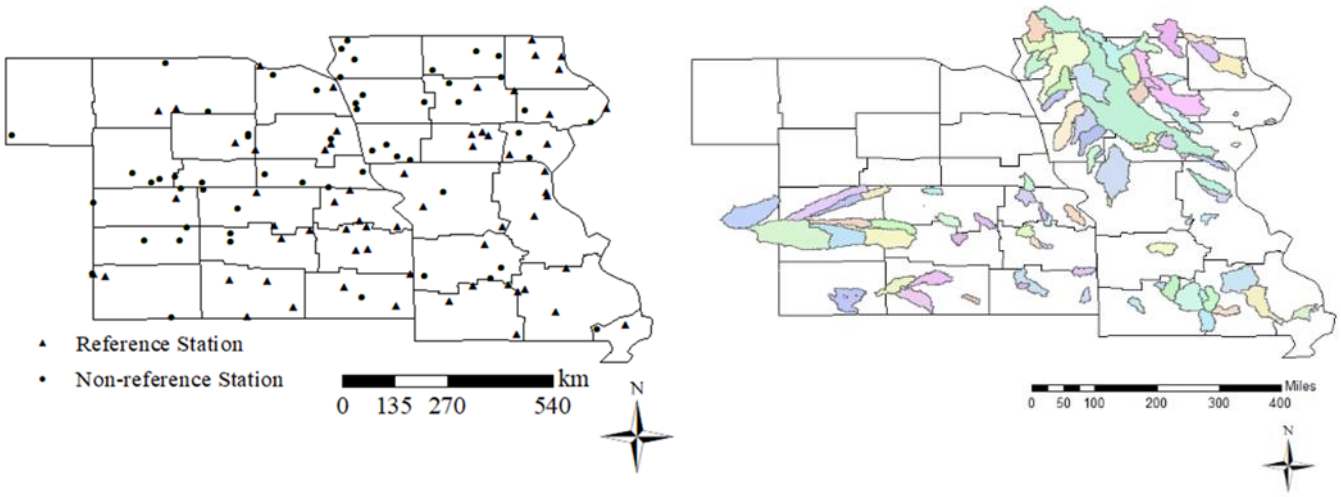

Figure 3-2 Watershed information 2a) climate division boundaries and location of all USGS stream gauges used in the study, 2b) watershed sizes of gauges for Missouri, Iowa, and Kansas.

The table below summarizes the watersheds used in this analysis (detailed watershed table in appendix A). The count is the total number of watersheds though the land cover related fields do not include Nebraska watersheds and some in the other states. The smallest and largest show the size range of single watersheds used in the region and each state.

Table 3-1 Summary of watersheds sizes and state land cover information.

Watershed Summary					
	MINK	**Kansas**	**Nebraska**	**Iowa**	**Missouri**
Count	117	34	25	36	22
Smallest (sq. km)	66	253	113	66	169
Largest (sq. km)	221,703	66,726	149,313	221,703	36,260
Smallest Land cover	Deciduous Forest	Deciduous Forest	NA	Grass/Herbaceous	Grass/Herbaceous
Average Area (%)	11	4	NA	4	1
Largest Land cover	Cultivated Crop	Grass/Herbaceous	NA	Cultivated Crop	Deciduous Forest
Average Area (%)	40	40	NA	68	36

Results and Discussion

Comparing Drought Indices to Land Cover on Climate Division Scale

Working at the climate division scale the remote sensing drought indices (VCI and SMCI) were compared to the area of major land cover types in order to understand the effect

land cover has on the performance analysis of each index. Most of the MINK region is dominated by agriculture (cropland and pasture) with scattered natural grasslands in the west and forest primarily in southern Missouri (Fig. 3-1a). The main land covers by percentage of area in the MINK region are cultivated cropland (40%), grassland and herbaceous (26%), pasture and hay (13%), and deciduous forest (11%).

To compare each index to cropland, the percentage of cropland was calculated for each climate division. The 15-year average value for each drought indicator was calculated to be directly compared to cropland amount. The results address what drought index value would one expect to see depending on the amount of a certain land cover (%). Initially, the analysis was only conducted with cultivated cropland (the most dominant land cover type) to see how each index performed. It was expected that VCI would have the highest correlations with Percent Cultivated Cropland since VCI estimates vegetation greenness. It was hypothesized that SMCI would show fairly strong correlations. The hypothesis was partially correct as VCI does have the highest correlation with cultivated cropland as seen in Figure 3-4. Surprisingly, SMCI had a low coefficient of determination (R^2<0.1) with cultivated cropland. SMCI showed a low to fair relationship with the other land cover types as shown in Figure 3-3. Before running the analysis, it was hypothesized that SMCI would have a fairly strong relationship with land cover since SMCI uses soil moisture as an input, which influences crop growth. It is possible that because the scale is so large (climate division basis), soil moisture conditions are influenced by a wide variety of factors like precipitation variation, irrigated land, or varying soil types. Since the SMCI calculated for this study uses soil moisture from the top 10 cm of soil depth, it is also possible that it is not a good indicator of crop coverage, since the plant root depth extends far lower than the top 10 cm. SMCI performed best with the grassland and herbaceous cover type,

followed by pasture and hay cover. A study that evaluated satellite derived soil moisture in relation to drought and land cover found that grassland areas showed a stronger response to soil moisture drought than forested areas (Nicolai-Shaw, Zscheischler, Hirschi, Gudmundsson, & Seneviratne, 2017). The reason behind SMCI performing best in grasslands was looked at in a study analyzing different remotely sensed soil moisture products in France. The study explained that remotely sensed soil moisture should be retrievable with high accuracy in herbaceous land cover (Rudiger, *et al.*, 2009).

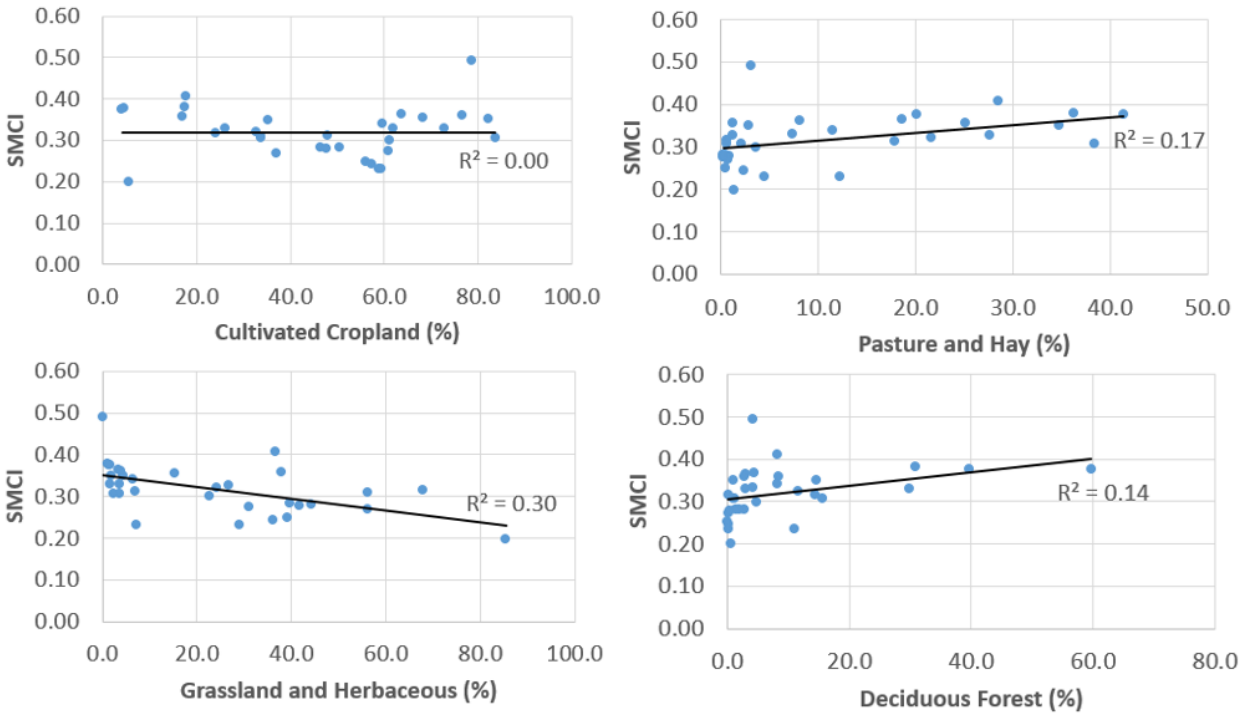

Figure 3-3 Graphs showing the relationship between each dominant land cover type (cultivated cropland, pasture and hay, grassland and herbaceous, and deciduous forest) in the MINK region with SMCI.

Since VCI had a fairly moderate relationship with cultivated cropland (R^2 = 0.4) the same analysis was performed for three different land cover types (deciduous forest, pasture and hay, and grassland and herbaceous). The graphs for VCI against each cover type are shown in Figure 3-4 below. The graphs show that: as the percentage of grassland and herbaceous cover increases

within a climate division, the average VCI decreases (R^2 = 0.18); as the percent of pasture and hay increases, average VCI increases within a climate division (R^2 = 0.73); and as the percent deciduous forest increases, average VCI also increases (R^2 = 0.65). The deciduous forest relationship does not seem to be a direct linear relationship, as it tends to level off as the percent land cover increases. It was predicted that climate divisions with more forest would have higher average VCI due to forests having such a dense greenness that increases NDVI (VCI) as the amount of forest coverage increases.

A surprising finding from this analysis is that average VCI decreases for both cultivated cropland and grassland and herbaceous as the percentage of each cover type increases, which could be due to using season averages as opposed to peak VCI values. Both relationships also had the lowest R^2 values. VCI has been shown to have the best correlations with other drought indices in grassy regions compared to lower correlations in forested or cropland areas (Zhang, Jiao, Zhang, Huang, & Tong, 2017). The results of chapter 2 show that VCI performs best in the western part of the MINK region (Kansas and Nebraska), which is primarily grassland and cultivated cropland. VCI performed best in the semi-arid (western) region of Texas, which is similar to the western parts of Kansas and Nebraska (Quiring & Ganesh, 2010). Figure 4 shows that VCI has a relatively weak relationship with grassland compared to the other cover types.

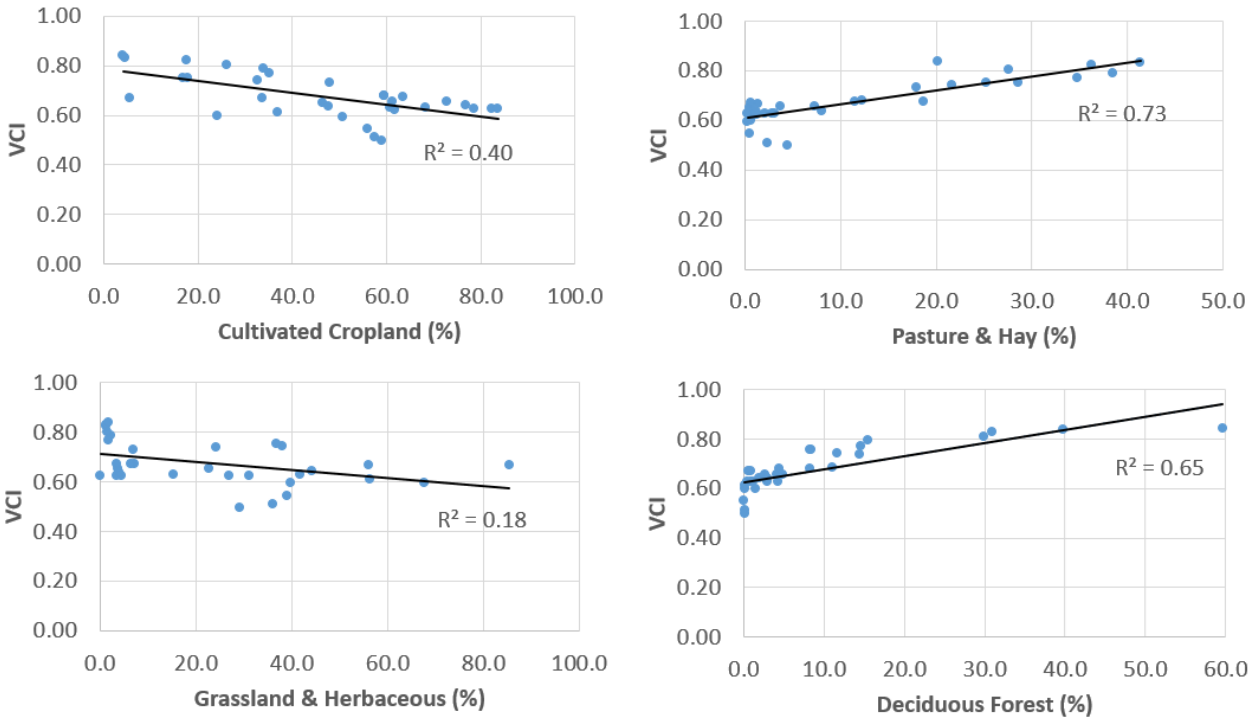

Figure 3-4 Graphs showing the relationships between each land cover type (cultivated cropland, pasture and hay, grassland and herbaceous, and deciduous forest) with VCI.

These finding show that in fact on a large scale (climate division basis) the results from chapter 2 that included VCI may be influenced by land cover type. The relationship between pasture and hay and deciduous forest with VCI are fairly strong from a statistical perspective while VCI's relationship with cultivated cropland and grassland and herbaceous land cover seems to be weaker. SMCI shows a fair relationship with land cover overall, though its relationship with cultivated cropland is weak.

Comparing Remote Sensing Indices to Land Cover on Watershed Scale

To get a better understanding of how the drought indices (SMCI, VCI) are influenced by land cover on a smaller scale, a similar analysis was conducted on an individual watershed scale. This will allow analysis of how land cover can affect the remote sensing indicators (SMCI, VCI) relationships with PDA in the previous analysis, since PDA is watershed based and not climate division based. The indices had to be determined for each specific watershed. This is possible

since the raw remote sensing indicator values were on a pixel basis, which were then aggregated on a climate division basis to be compared to land cover in the previous analysis. For this part, the drought indices (SMCI, VCI) were aggregated to individual watersheds where discharge data was obtained in order to calculate PDA. Only watersheds from Iowa, Kansas, and Missouri were used in this part of the study, since Nebraska watershed boundary information was unavailable from USGS.

Figure 3-5 helps visualize the relationships at the watershed scale between each dominant land cover type in the region and SMCI. Results show that the relationships between land cover and SMCI are weaker overall compared to the climate division scale. The strongest relationship is weak, with an $R^2 = 0.08$ for grassland and herbaceous cover. Due to the increase in the number of data points, the variability in the data has increased drastically, which contributes to a weaker relationship. Though the relationships between SMCI and land cover types on a watershed scale are weak the overall trends are similar. SMCI tends to perform best with other drought indices in areas with less tree coverage like grasslands and croplands (Zhang, Jiao, Zhang, Huang, & Tong, 2017).

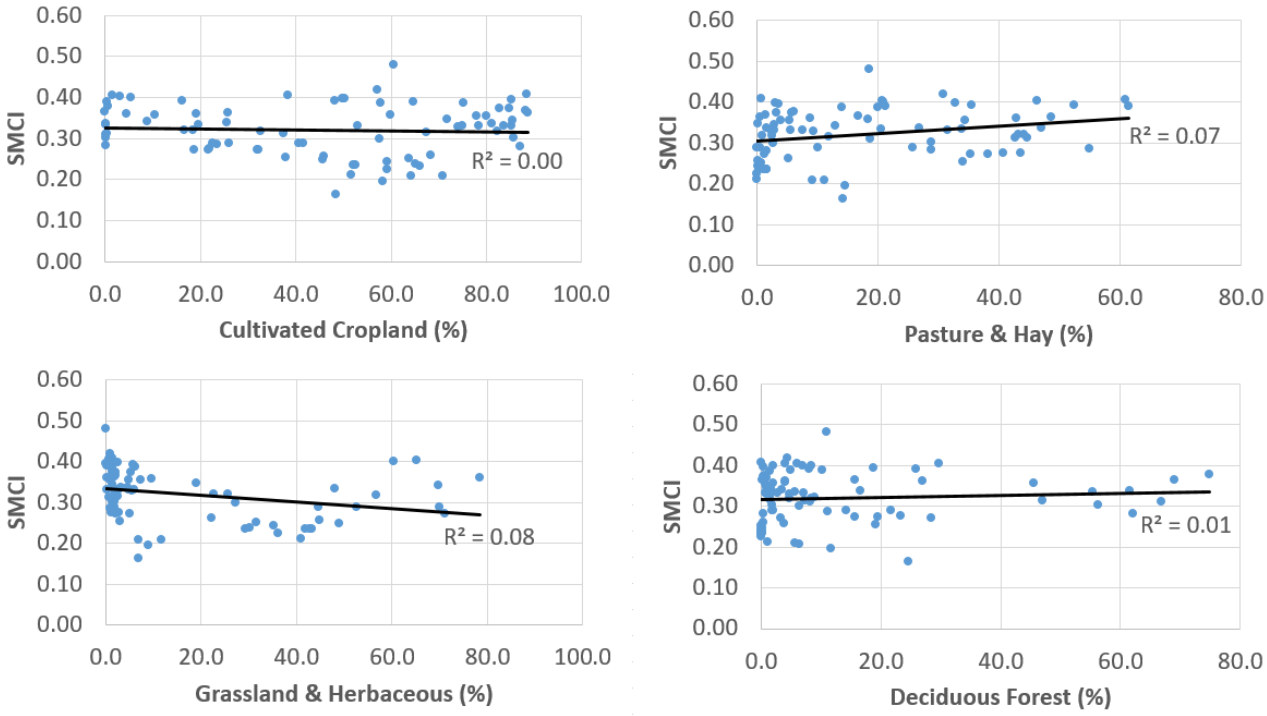

Figure 3-5 Graphs showing the relationship between average SMCI on a watershed scale and each land cover type percentage (cultivated cropland, pasture and hay, grassland and herbaceous, and deciduous forest), N = 85.

VCI had fair to strong relationships with each land cover type on a climate division scale, so it was predicted that the relationships would be similar at the watershed scale. For the most part, this is true. Figure 6 illustrates the relationships between VCI and land cover types are fairly strong in pasture and hay (R^2 = 0.52), deciduous forest (R^2 = 0.47), and cultivated cropland (R^2 = 0.46) while fairly weak in grassland and herbaceous (R^2 = 0.11) for the 85 watersheds analyzed.

Surprising, coefficient of determination values for VCI dropped significantly from the climate division analysis for the top two land cover types (pasture and hay and deciduous forest) while cultivated cropland increased from R^2 = 0.40 to R^2 = 0.46. The trends are similar, which suggests that as the percentage of pasture and hay and deciduous forest increase, the average VCI also increases. On the other hand, when the percentage of cropland and grassland and herbaceous increase, the average VCI decreases. VCI has shown to perform best in grassland and cropland

regions as discussed in part 1 of this analysis, but VCI's relationship with land cover could be influenced by precipitation variation as well. For a study conducted in Kansas, it was found that NDVI (input for VCI) had the highest correlations in forest areas and lower correlations in cropland areas (Wang, Price, & Rich, 2001). This claim is similar with the results of this study, showing that there are a variety of conclusions between the relationship of land cover and vegetation drought indices (VCI, NDVI).

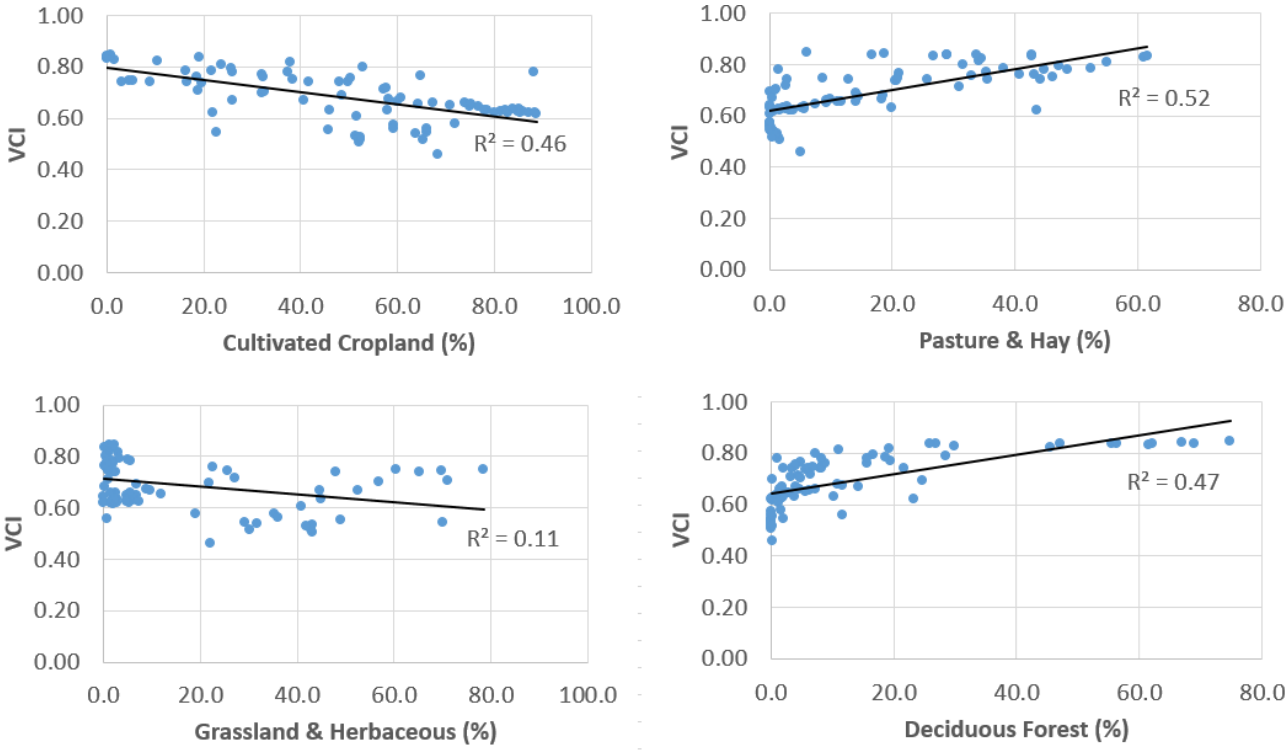

Figure 3-6 Graphs showing the relationship between average VCI on a watershed scale and land cover percentage (cultivated cropland, pasture and hay, grassland and herbaceous, and deciduous forest), N= 85.

This analysis confirms that VCI is influenced by land cover types while SMCI is also related to land cover, though not as strongly as VCI. Knowing how VCI and SMCI are influenced by varying land covers is useful to know when making conclusions on just how these indices relate to the *in situ* indices (PDSI, SPI) and PDA.

Conclusions

The first part of this study looked at the large-scale effects (climate division scale) of land cover on the drought indices. SMCI had the smallest R^2 value with cultivated cropland (essentially 0). The other land covers (grassland and herbaceous, pasture and hay, and deciduous forest) had stronger relationships with SMCI, though still relatively weak. For the VCI index, the greatest influence from land cover was for cultivated cropland (R^2 = 0.40). VCI was evaluated against the next three dominant land cover types in the region (grassland and herbaceous, deciduous forest, and pasture and hay) with moderately low to high R^2 values for each type (R^2 = 0.18, 0.65, and 0.73 respectively).

The second part of this study looked at verifying the effects of land cover at the watershed scale for both SMCI and VCI. The results verified the initial findings as R^2 values remained below 0.1 for SMCI in each land cover type while moderate R^2 values (greater than 0.45) for VCI were found for all land cover types except grassland and herbaceous. Interestingly the R^2 values varied between climate division scale and watershed scale, which could be due to local variability and an increase in the number of data points.

These results suggest that land cover does influence VCI. This finding agrees with other studies, which have shown that deforestation and crop rotation have falsely reported drought conditions and reduce accuracy with VCI monitoring (Yagci, Di, & Deng, 2014). For both cultivated cropland and grassland and herbaceous, VCI tended to decrease with a higher percentage of each cover type. For pasture and hay and deciduous forest, VCI tended to increase as the percentage of these two cover types increased. SMCI was shown to also be influenced by land cover with low correlations. This work helps to verify the influences that land cover can have on the remote sensing drought indices (SMCI, VCI) and then being able to predict

streamflow (PDA) changes. The finding that VCI is strongly influenced by land cover could explain why VCI had the weakest relationships with PDA across the region, since PDA is mainly influenced by meteorological conditions (precipitation and temperature) and not land cover. Since SMCI had little correlation with land cover characteristics, this finding could explain why SMCI performed better in predicting PDA.

Chapter 4 - Summary and Conclusion

The goal of this study was to answer the question: can remote sensing drought indices (*e.g.* VCI and SMCI) be used to monitor streamflow changes as effectively as *in situ* drought indices (*e.g.* PDSI and SPI)? To address this question, linear regression analyses were conducted to test for differences. The remote sensing indices were compared to the *in situ* indices over the four-state MINK region. Each index was also compared to streamflow changes (by PDA) to determine how well each drought index correlates with changes in streamflow. Finally, and to test for the effect that land cover has on these relationships, the remote sensing indices were assessed for the different land cover types in the region.

The indices were compared spatially on a climate division scale for the entire region. Results indicated that SMCI performed better than VCI overall when compared to PDSI and SPI over the region, with shorter-time scale SPIs (1-3 month) having the highest correlations with SMCI. This finding agrees with other studies that showed SMCI performs best with short-term drought (Zhang, Jiao, Zhang, Huang, & Tong, 2017). On the other hand, VCI performed best overall with SPI-2 and showed stronger correlations with SPI and PDSI in the western part of the study region (western Nebraska and Kansas). Other research suggests that VCI performs best in semi-arid areas (southern and southwest United States) when compared to PDSI and SPI (Quiring & Ganesh, 2010).

Each drought index was compared to PDA for 117 stream gauge stations scattered throughout the MINK region. Due to their inputs (precipitation data), the *in situ* drought indices (PDSI and SPI) were predicted to perform better in monitoring PDA and have shown to be able to monitor streamflow changes (Zhai, *et al.*, 2010). SPI-3 ($R^2 = 0.49$) and PDSI ($R^2 = 0.48$) indicated stronger power for predicting PDA in the MINK region than any other index. SMCI

showed stronger performance (R^2 = 0.38) in monitoring PDA than VCI (R^2 = 0.19) within the region. Although VCI had an overall weak relationship, it showed higher R^2 values with PDA in the western states of Kansas (R^2 = 0.32) and Nebraska (R^2 = 0.24).

In a comparison of reference and non-reference stream gauges throughout the region, the reference streamflow station-based PDAs had higher correlations with all drought indices (except SPI-24). This was expected, as reference gauges have stronger correlations with natural phenomena like drought (Lorenzo-Lacruz, *et al.*, 2010). Overall, both remotely sensed indices (VCI, SMCI) did not perform as well as the *in situ* indices (PDSI, SPI) in predicting PDA within the region.

To assess the effects that land cover might have on the results of chapter 2, chapter 3 addressed the relationship between land cover and each drought index. Four dominant land cover types in the region (cultivated cropland, pasture and hay, grassland and herbaceous, and deciduous forest) were used and their area percentage was compared to each drought index (VCI and SMCI). Results suggest that land cover has a minor effect on SMCI, which could be due to soil moisture being influenced by other factors including precipitation and irrigation. VCI on the other hand showed stronger relationships with land cover, with R^2 values as high as 0.45 for cultivated cropland, pasture and hay, and deciduous forest cover types. The effect of land cover on the correlations between the remote sensing indices (VCI and SMCI) and PDA could very well be a factor in explaining why VCI and SMCI has a weaker relationship with PDA compared to PDSI and SPI. The results indicate VCI could most definitely be influenced by land cover type, which might suggest why VCI performs differently depending on the region.

The results of this study can benefit the individuals and organizations that monitor drought and streamflow. Such organizations include national agencies like the Environmental

Protection Agency (EPA), United States Geological Survey (USGS), and United States Army Corps of Engineers (USACE) and state-based organizations such as the Kansas Department of Health and Environment (KDHE) and the Kansas Water Office (KWO). These organizations could use results from this study to determine which indices to use when monitoring drought or streamflow changes. Other people that benefit from these results include those from places that do not have regular access to station-based data to monitor streamflow or *in situ* drought indices. Satellite data is readily available across the globe on various websites like those supported by NASA. Working within a geographic information system or image processing software package, the satellite image data can be converted into either vegetation or soil moisture indices. Using remotely sensed drought indices such as VCI and SMCI in places that do not have regular access to stream gauge station data is the main motivation behind this work.

A future step to this work could be to analyze other remotely sensed indices. Subsequent work might use remotely sensed precipitation data or incorporate rainfall estimates from radar return signals. Another option might be to incorporate more variables into a multi-variate statistical approach. If a newly developed index was as highly correlated with PDA as SPI or PDSI, then areas that do not have access to stream gauge stations could use such an index instead. In the meantime, SMCI could cautiously be used to a degree to monitor streamflow, though it is more limited than using PDSI or SPI.

Chapter 5 - References

AghaKouchak, A., Farahmand, A., Melton, F. S., Teixeira, J., Anderson, M. C., Wardlow, B. D., & Hain, C. R. (2015). Remote sensing of drought: Progress, challenges and opportunities. *Reviews of Geophysics*, 452-480.

Ahiablame, L., Sheshukov, A. Y., Rahmani, V., & Moriasi, D. (2017). Annual baseflow variations as influenced by climate variability and agricultural land use change in the Missouri River Basin. *Journal of Hydrology*, 188-202.

Alley, W. M. (1984). The Palmer Drought Severity Index: Limitations and Assumptions. *Journal of Climate and Applied Meteorology* , 1100-1109.

Anderson, M. C., Hain, C., Wardlow, B., Pimstein, A., & Mecikalski, J. R. (2011). Evaluation of Drought Indices Based on Thermal Remote Sensing of Evapotranspiration over the Continental United States. *Journal of Climate*, 2025-2044.

Bandad, D., & Rahmani, V. (2018). Analysis of PDSI and Vegetation Condition Index (VCI) and Their Links to Streamflow. *American Society of Agricultural and Biological Engineers*, 1-8.

Bandad, D., & Rahmani, V. (2019). Capability of Remote-Sensing and In Situ Drought Indices for Detecting Drought and Streamflow in the MINK Region from 2003-2017. *American Society of Agricultural and Biological Engineers*, 1-5.

Easterling, W. E., Crosson, P. R., Rosenberg, N. J., McKenney, M. S., Katz, L. A., & Lemon, K. M. (1993). Paper 2. Agricultural Impacts of and Responses to Climate Change in the Missouri- Iowa- Nebraska- Kansas (MINK) Region. *Climatic Change*, 23-61.

Frederick, K. D. (1993). Paper 4. Climate Change Impacts on Water Resources and Possible Responses in the MINK Region. *Climate Change*, 83-115.

Guttman, N. B. (1998). Comparing the Palmer Drought Index and the Standardized Precipiation Index. *Journal of the American Water Resources Association* , 113-121.

Hao, C., Zhang, J., & Yao, F. (2015). Combination of multi-sensor remote sensing data for droughtmonitoring over Southwest China. *International Journal of Applied Earth Observation and Geoinformation* , 270-283.

Haslinger, K., Koffler, D., Schoner, W., & Laaha, G. (2014). Exploring the link between meteorological drought and streamflow: Effects of climate-catchment interaction. *Water Resources Research*, 2468-2487.

Heim Jr., R. R. (2002). A Review of Twentieth Century Drought Indices Used in the United States. *American Meteorological Society*, 1149-1166.

Irrigation & Water Use. (2019, April 1). Retrieved from United States Department of Agriculture Economic Research Service: https://www.ers.usda.gov/topics/farm-practices-management/irrigation-water-use/

Jiao, W., Zhang, L., Chang, Q., Fu, D., Cen, Y., & Tong, Q. (2016). Evaluating an Enhanced Vegetation Condition Index (VCI) Based on VIUPD for Drought Monitoring in the Continental United States. *Remote Sensing*, 1-21.

Karl, T. A. (1986). The Sensitivity of the Palmer Drought Severity Index and Palmer's Z-Index to their Calibration Coefficients Including Potential Evapotranspiration. *Journal of Climate and Applied Meteorology* , 77-86.

Kogan, F. (1990). Remote sensing of weather impacts on vegetation in non-homgeneous areas. *International Journal of Remote Sensing*, 1405-1419.

Li, X., He, B., Quan, X., Liao, Z., & Bai, X. (2015). Use of the Standardized Precipitation Evapotranspiration Index (SPEI) to Characterize the Drying Trend in Southwest China from 1982–2012. *Remote Sensing*, 10917-10937.

Liu, W., Cai, T., Fu, G., Zhang, A., Liu, C., & Yu, H. (2013). The streamflow trend in Tangwang River basin in northeast China and its difference response to climate and land use change in sub-basins. *Environmental Earth Science*, 51-62.

Lorenzo-Lacruz, J., Vicente-Serrano, S., López-Moreno, J., Beguería, S., García-Ruiz, J., & Cuadrat, J. (2010). The impact of droughts and water management on various hydrological systems in the headwaters of the Tagus River (central Spain). *Journal of Hydrology*, 13-26.

McKee, T. B., Doesken, N. J., & Kleist, J. (1993). The Relationship of Drought Requency and Duration to Time Scales. *8th Conference of Applied Climatology* (pp. 179-184). Anaheim, CA: American Meteorological Society.

Nicolai-Shaw, N., Zscheischler, J., Hirschi, M., Gudmundsson, L., & Seneviratne, S. I. (2017). A drought event composite analysis using satellite remote-sensing based soil moisture. *Remote Sensing of Environment*, 1-10.

NOAA. (2019). *NOAA Climate*. Retrieved from climate: https://www.climate.gov/maps-data/data-snapshots/averagemaxtemp-monthly-1981-2010-cmb-0000-07-00?theme=Temperature

Otkin, J. A., Anderson, M. C., Hain, C., Svoboda, M., Johnson, D., Mueller, R., . . . Brown, J. (2016). Assessing the evolution of soil moisture and vegetation conditionsduring the 2012 United States flash drought. *Agricultural and Forest Meteorology*, 230-242.

Palmer, W. (1965). Meteorological Drought. *Research Paper No. 45. U.S. Weather Bureau, Washington, DC*, 1-58.

Piao, S., Fang, J., Zhou, L., Guo, Q., Henderson, M., Ji, W., . . . Tao, S. (2003). Interannual variations of monthly and seasonal normalized difference vegetation index (NDVI) in China from 1982 to 1999. *Journal of Geophysical Research* , 1-13.

Quiring, S. M., & Ganesh, S. (2010). Evaluating the utility of the Vegetation Condition Index (VCI) for monitoring meteorological drought in Texas. *Agricultural and Forest Meteorology*, 330-339.

Quiring, S. M., & Papakryiakou, T. N. (2003). An evaluation of agricultural drought indices for the Canadian prairies . *Agricultural and Forest Meteorology* , 49-62.

Rahmani, V., Hutchinson, S. L., Harrington Jr, J. A., Hutchinson, J. M., & Anandhi, A. (2015). Analysis of temporal and spatial distribution and change-points for annual precipitation in Kansas, USA. *International Journal of Climatology* , 3879-3887.

Rahmani, V., Hutchinson, S. L., Harrington Jr, J. A., Hutchinson, J. M., & Anandhi, A. (2015). Analysis of temporal and spatial distribution and change-points for annual precipitation in Kansas, USA. *International Journal of Climatology*, 3879-3887.

Rahmani, V., Kastens, J. J., DeNoyelles, F., Jakubauskas, M. E., Martinko, E. A., Huggins, D. H., . . . Blackwood, A. J. (2018). Examining Storage Capacity Loss and Sedimentation Rate of Large Reservoirs in the Central U.S. Great Plains. *Water*, 1-17.

Ren, L., Wang, M., Li, C., & Zhang, W. (2002). Impacts of human activity on river runoff in the northern area of China. *Journal of Hydrology*, 204-217.

Rudiger, C., Calvet, J.-C., Gruhier, C., Holmes, T. R., De Jeu, R. A., & Wagner, W. (2009). An Intercomparison of ERS-Scat and AMSR-E Soil Moisture Observations with Model Simulations over France. *Journal of Hydrometeorology* , 431-447.

Svoboda, M., & Fuchs, B. A. (2016). *Handbook of Drought Indicators and Indices.* Geneva: World Meteorological Organization (WMO) and Global Water Partnership (GWP).

Tarpley, J., Schneider, S., & Money, R. (1984). Global Vegetation Indices from the NOAA-7 Meteorological Satellite. *Journal of Climate and Applied Meteorology*, 491-494.

Tavakol, A., Rahmani, V., Quiring, S. M., & Kumar, S. V. (2019). Evaluation analysis of NASA SMAP L3 and L4 and SPoRT-LIS soil moisture data in the United States. *Remote Sensing of Environment* , 234-246.

Tucker, C. J. (1979). Red and photographic infrared linear combinations for monitoring vegetation. *Remote Sensing of Environment*, 127-150.

Vicente-Serrano, S. M. (2007). Evaluating the Impact of Drought Using Remote Sensing in a Mediterranean, Semi-arid Region. *Natural Hazards*, 173-208.

Vicente-Serrano, S. M., Begueri´a, S., Lorenzo-Lacruz, J., Julio Camarero, J. s., Lo´pez-Moreno, J. I., Azorin-Molina, C., . . . Sanchez-Lorenzo, A. (2012). Performance of Drought

Indices for Ecological, Agricultural, and Hydrological Applications. *Earth Interactions* , 1-27.

Vose, R. S., Applequist, S., Squires, M., Durre, I., Menne, M. J., Williams Jr, C. N., . . . Arndt, D. (2014). Improved Historical Temperature and Precipitation Time Series for U.S. Climate Divisions. *Journal of Applied Meteorology and Climatology*, 1232-1251.

Wang, J., Price, K. P., & Rich, P. M. (2001). Spatial patterns of NDVI in response to precipitation and temperature in the central Great Plains. *International Journal of Remote Sensing*, 3827-3844.

Wen, L., Rogers, K., Ling, J., & Saintilan, N. (2011). The impacts of river regulation and water diversion on the hydrological drought characteristics in the Lower Murrumbidgee River, Australia. *Journal of Hydrology*, 382-391.

Yagci, A. L., Di, L., & Deng, M. (2014). THE INFLUENCE OF LAND COVER-RELATED CHANGES ON THE NDVI-BASED SATELLITE AGRICULTURAL DROUGHT INDICES . *IEEE*, 2054-2057.

Zargar, A., Sadiq, R., Naser, B., & Khan, F. I. (2011). A Review of Drought Indices . *Environmental Reviews* , 333-349.

Zhai, J., Su, B., Krysanova, V., Vetter, T., Gao, C., & Jiang, T. (2010). Spatial Variation and Trends in PDSI and SPI Indices and Their Relation to Streamflow in 10 Large Regions of China. *Journal of Climate*, 649-663.

Zhang, A., & Jia, G. (2013). Monitoring Meteorological Drought in Semiarid Regions using Multi-Sensor Microwave Remote Sensing Data. *Remote Sensing of Environment* , 12-23.

Zhang, L., Jiao, W., Zhang, H., Huang, C., & Tong, Q. (2017). Studying drought phenomena in the Continental United States in 2011 and 2012 using various drought indices. *Remote Sensing of Environment*, 96-106.

Zhao, G., Tian, P., Mu, X., Jiao, J., Wang, F., & Gao, P. (2014). Quantifying the impact of climate variability and human activities on streamflow in the middle reaches of the Yellow River basin, China. *Journal of Hydrology*, 387-398.

Zhao, L., Lyu, A., Wu, J., Hayes, M., Tang, Z., He, B., . . . Liu, M. (2014). Impact of meteorological drought on streamflow drought in Jinghe River Basin of China. *Chinese Geographical Science*, 694-705.

Appendix A - Watershed and PDA Relationship Table

STAID	Station Name	CLASS	Drain Area (km^2)	VCI (R^2)	SMCI (R^2)	PDSI (R^2)	SPI_1 (R^2)	SPI_2 (R^2)	SPI_3 (R^2)	SPI_6 (R^2)	SPI_9 (R^2)	SPI_12 (R^2)	SPI_24 (R^2)
5387440	Upper Iowa River at Bluffton, IA	Ref	951	0.04	**0.36**	0.20	**0.59**	**0.56**	**0.52**	**0.54**	**0.56**	**0.34**	0.01
5389400	Bloody Run Creek near Marquette, IA	Ref	88	0.00	**0.27**	**0.41**	**0.44**	**0.50**	**0.52**	**0.52**	**0.54**	**0.50**	0.20
5411850	Turkey River near Eldorado, IA	Ref	1660	0.08	0.24	0.16	**0.33**	**0.36**	**0.34**	**0.31**	**0.31**	0.20	0.00
5412500	Turkey River at Garber, IA	Ref	4002	0.03	**0.35**	**0.40**	**0.51**	**0.55**	**0.58**	**0.52**	**0.56**	**0.46**	0.07
5420460	Beaver Slough at 3rd Street at Clinton, IA	Non-ref	221704	0.00	0.00	0.17	0.18	0.14	0.19	0.21	0.18	0.16	0.18
5422600	Duck Creek at DC Golf Course at Davenport, IA	Non-ref	148	0.01	**0.40**	**0.58**	**0.58**	**0.65**	**0.63**	**0.62**	**0.65**	**0.59**	0.23
5451210	South Fork Iowa River NE of New Providence, IA	Ref	580	0.01	**0.67**	**0.68**	**0.81**	**0.79**	**0.72**	**0.57**	**0.69**	**0.62**	0.21

5453100	Iowa River at Marengo, IA	Non-ref	7236	0.02	**0.51**	**0.60**	**0.74**	**0.66**	**0.67**	**0.57**	**0.53**	**0.47**	0.18
5454000	Rapid Creek near Iowa City, IA	Ref	66	0.02	**0.47**	**0.71**	**0.74**	**0.75**	**0.69**	**0.59**	**0.61**	**0.56**	**0.38**
5457700	Cedar River at Charles City, IA	Non-ref	2730	0.03	0.22	0.14	**0.26**	**0.32**	**0.33**	0.23	0.15	0.09	0.01
5459500	Winnebago River at Mason City, IA	Non-ref	1362	0.08	**0.37**	**0.32**	**0.50**	**0.52**	**0.52**	**0.53**	**0.49**	**0.27**	0.01
5463000	Beaver Creek at New Hartford, IA	Non-ref	899	0.02	**0.29**	**0.27**	**0.39**	**0.44**	**0.44**	**0.30**	**0.32**	0.18	0.02
5464220	Wolf Creek near Dysart, IA	Ref	774	0.01	**0.52**	**0.70**	**0.65**	**0.75**	**0.81**	**0.79**	**0.75**	**0.58**	**0.29**
5471000	South Skunk River below Squaw Creek near Ames, IA	Non-ref	1440	0.00	**0.71**	**0.63**	**0.81**	**0.79**	**0.75**	**0.51**	**0.52**	**0.43**	0.18
5472500	North Skunk River near Sigourney, IA	Non-ref	1891	0.01	**0.60**	**0.79**	**0.74**	**0.77**	**0.85**	**0.86**	**0.83**	**0.66**	**0.37**
5473450	Big Creek North of Mount Pleasant, IA	Ref	150	0.00	**0.72**	**0.87**	**0.78**	**0.81**	**0.85**	**0.77**	**0.80**	**0.77**	**0.50**

5479000	East Fork Des Moines River at Dakota City, IA	Non-ref	3388	0.10	**0.44**	0.19	**0.34**	**0.31**	**0.27**	0.10	0.17	0.20	0.01
5481000	Boone River near Webster City, IA	Non-ref	2186	0.00	**0.61**	**0.45**	**0.64**	**0.60**	**0.55**	**0.35**	**0.43**	**0.39**	0.06
5482500	North Raccoon River near Jefferson, IA	Non-ref	4193	0.05	**0.60**	**0.46**	**0.55**	**0.59**	**0.67**	**0.48**	**0.51**	**0.44**	0.08
5487980	White Breast Creek near Dallas, IA	Ref	862	0.00	**0.48**	**0.68**	**0.59**	**0.70**	**0.78**	**0.85**	**0.74**	**0.47**	0.15
5488200	English Creek near Knoxville, IA	Ref	233	0.05	**0.65**	**0.71**	**0.81**	**0.83**	**0.85**	**0.75**	**0.69**	**0.46**	0.22
5489000	Cedar Creek near Bussey, IA	Ref	969	0.00	**0.47**	**0.71**	**0.53**	**0.63**	**0.72**	**0.81**	**0.74**	**0.51**	0.23
5490500	Des Moines River at Keosauqua, IA	Non-ref	36358	0.00	**0.67**	**0.76**	**0.75**	**0.75**	**0.81**	**0.75**	**0.79**	**0.72**	**0.39**
5494300	Fox River at Bloomfield, IA	Ref	227	0.00	**0.61**	**0.73**	**0.59**	**0.69**	**0.77**	**0.78**	**0.78**	**0.70**	**0.32**
5495000	Fox River at Wayland, MO	Ref	1036	0.17	**0.57**	**0.75**	**0.61**	**0.58**	**0.64**	**0.65**	**0.70**	**0.55**	**0.29**

5500000	South Fabius River near Taylor, MO	Ref	1606	0.04	**0.32**	**0.52**	**0.32**	**0.38**	**0.50**	**0.63**	**0.60**	**0.37**	0.01
5501000	North River at Palmyra, MO	Ref	917	0.08	**0.38**	**0.60**	**0.41**	**0.48**	**0.58**	**0.71**	**0.66**	**0.40**	0.03
5506100	Long Branch near Santa Fe, MO	Ref	466	0.15	**0.51**	**0.48**	**0.45**	**0.57**	**0.58**	**0.61**	**0.55**	**0.37**	0.07
6453600	Ponca Creek at Verdel, Nebr.	Ref	2103	0.03	0.19	**0.47**	0.15	0.19	0.25	0.23	**0.33**	**0.40**	**0.38**
6461500	Niobrara River near Sparks, Nebr.	Non-ref	18519	**0.76**	**0.39**	**0.57**	**0.49**	**0.49**	**0.54**	**0.42**	**0.44**	**0.45**	0.25
6466400	Bazile Creek at Center, Nebr.	Non-ref	0	0.08	**0.33**	**0.61**	**0.32**	**0.35**	**0.38**	0.24	**0.35**	**0.42**	**0.38**
6483290	Rock River below Tom Creek at Rock Rapids, IA	Non-ref	2209	**0.35**	0.10	**0.26**	0.03	0.03	0.03	0.00	0.04	0.22	**0.33**
6483500	Rock River near Rock Valley, IA	Non-ref	4123	0.05	**0.50**	**0.49**	**0.35**	**0.37**	**0.45**	0.25	**0.43**	**0.46**	0.14
6600100	Floyd River at Alton, IA	Non-ref	694	0.06	**0.43**	**0.36**	**0.51**	**0.56**	**0.61**	**0.52**	**0.60**	**0.42**	0.12
6600500	Floyd River at James, IA	Non-ref	2295	**0.40**	**0.31**	**0.47**	0.12	0.11	0.11	0.04	0.20	**0.38**	**0.37**

6601000	Omaha Creek at Homer, Nebr.	Ref	451	0.11	**0.30**	**0.63**	**0.40**	**0.41**	**0.42**	**0.33**	**0.51**	**0.62**	**0.34**
6607200	Maple River at Mapleton, IA	Non-ref	1733	0.08	**0.66**	**0.75**	**0.69**	**0.67**	**0.70**	**0.57**	**0.73**	**0.79**	**0.35**
6607500	Little Sioux River near Turin, IA	Non-ref	9132	0.10	**0.40**	**0.44**	**0.34**	**0.34**	**0.35**	0.23	**0.35**	**0.44**	0.23
6608500	Soldier River at Pisgah, IA	Non-ref	1054	0.07	**0.53**	**0.62**	**0.59**	**0.58**	**0.57**	**0.47**	**0.61**	**0.65**	**0.34**
6762500	Lodgepole Creek at Bushnell, Nebr.	Non-ref	3144	NA	NA	NA	NA	NA	NA	NA	NA	NA	NA
6770500	Platte River near Grand Island, Nebr.	Non-ref	149314	0.18	0.07	**0.29**	0.10	0.12	0.15	0.11	0.11	0.23	**0.30**
6775500	Middle Loup River at Dunning, Nebr.	Ref	4740	0.50	0.16	**0.29**	**0.26**	0.24	**0.26**	0.24	0.19	0.18	0.16
6775900	Dismal River near Thedford, Nebr.	Non-ref	2502	0.06	0.00	0.04	0.00	0.01	0.02	0.01	0.01	0.02	0.00
6784000	South Loup River at Saint Michael, Nebr.	Ref	6009	**0.51**	**0.68**	**0.88**	**0.42**	**0.52**	**0.55**	**0.39**	**0.56**	**0.65**	**0.58**

6785000	Middle Loup River at Saint Paul, Nebr.	Non-ref	20914	**0.54**	**0.76**	**0.75**	**0.55**	**0.67**	**0.75**	**0.58**	**0.63**	**0.59**	**0.42**
6786000	North Loup River at Taylor, Nebr.	Non-ref	6087	**0.53**	**0.49**	**0.83**	**0.48**	**0.56**	**0.63**	**0.52**	**0.57**	**0.56**	**0.35**
6790500	North Loup River near Saint Paul, Nebr.	Non-ref	11142	**0.42**	**0.53**	**0.77**	**0.35**	**0.47**	**0.56**	**0.47**	**0.55**	**0.59**	**0.54**
6796500	Platte River near Leshara, Nebr.	Non-Ref	0	0.12	**0.47**	**0.64**	**0.63**	**0.59**	**0.64**	**0.45**	**0.55**	**0.58**	**0.34**
6799445	Logan Creek at Wakefield, Nebr.	Non-ref	0	0.10	**0.32**	**0.53**	**0.48**	**0.50**	**0.51**	**0.33**	**0.49**	**0.55**	0.21
6803530	Rock Creek near Ceresco, Nebr.	Ref	311	0.08	**0.35**	**0.61**	**0.61**	**0.63**	**0.66**	**0.53**	**0.64**	**0.62**	**0.34**
6804000	Wahoo Creek at Ithaca, Nebr.	Non-ref	707	0.11	**0.41**	**0.76**	**0.62**	**0.61**	**0.65**	**0.61**	**0.75**	**0.81**	**0.53**
6808500	West Nishnabotna River at Randolph, IA	Non-ref	3434	0.00	**0.50**	**0.66**	**0.61**	**0.64**	**0.71**	**0.67**	**0.71**	**0.60**	**0.31**
6809500	East Nishnabotna River at Red Oak, IA	Non-ref	2315	0.03	**0.56**	**0.64**	**0.76**	**0.75**	**0.74**	**0.56**	**0.60**	**0.51**	**0.28**

6811500	Little Nemaha River at Auburn, Nebr.	Non-ref	2051	0.13	**0.38**	**0.73**	**0.50**	**0.50**	**0.51**	**0.41**	**0.58**	**0.73**	**0.51**
6814000	TURKEY C NR SENECA, KS	Ref	715	0.13	**0.33**	**0.37**	**0.41**	**0.42**	**0.46**	**0.47**	**0.52**	**0.39**	0.17
6817000	Nodaway River at Clarinda, IA	Non-ref	1974	0.01	**0.30**	**0.36**	**0.57**	**0.51**	**0.49**	**0.31**	**0.34**	**0.27**	0.12
6819185	East Fork 102 River at Bedford, IA	Non-ref	221	0.00	**0.54**	**0.44**	**0.64**	**0.60**	**0.58**	**0.39**	**0.45**	**0.46**	0.14
6819500	One Hundred and Two River at Maryville, MO	Non-ref	1334	0.14	**0.32**	**0.35**	**0.35**	**0.35**	**0.38**	**0.31**	**0.34**	0.22	0.00
6821080	Little Platte River near Plattsburg, MO	Ref	169	**0.30**	**0.49**	**0.61**	**0.49**	**0.51**	**0.45**	**0.36**	**0.46**	**0.59**	**0.31**
6827000	SF REPUBLICAN R NR CO-KS ST LINE, KS	Non-ref	4817	**0.26**	**0.30**	**0.66**	0.20	0.20	0.24	**0.32**	**0.38**	**0.38**	**0.58**
6834000	Frenchman Creek at Palisade, Nebr.	Non-ref	3367	**0.50**	**0.49**	**0.56**	**0.63**	**0.59**	**0.59**	**0.49**	**0.47**	**0.31**	0.14

6836500	Driftwood Creek near McCook, Nebr.	Non-ref	935	0.05	0.00	0.06	0.00	0.00	0.01	0.07	0.08	0.16	0.13
6838000	Red Willow Creek near Red Willow, Nebr.	Non-ref	2124	0.02	0.15	**0.37**	0.12	0.10	0.08	0.03	0.05	0.10	**0.38**
6843500	Republican River at Cambridge, Nebr.	Non-ref	37451	**0.31**	**0.36**	**0.46**	**0.47**	**0.40**	**0.42**	**0.43**	**0.49**	**0.43**	**0.26**
6844500	Republican River near Orleans, Nebr.	Non-ref	40352	**0.47**	**0.51**	**0.58**	**0.56**	**0.54**	**0.57**	**0.58**	**0.64**	**0.53**	**0.37**
6845110	SAPPA C NR LYLE, KS	Non-ref	3854	0.07	0.18	**0.42**	0.10	0.10	0.11	0.09	0.12	0.15	**0.35**
6847900	PRAIRIE DOG C AB KEITH SEBELIUS LAKE, KS	Ref	1528	0.21	0.19	**0.56**	0.19	0.18	0.20	**0.29**	**0.28**	**0.27**	**0.65**
6848500	PRAIRIE DOG C NR WOODRUFF, KS	Non-ref	2608	0.14	0.10	**0.54**	0.12	0.13	0.16	0.08	0.17	**0.28**	**0.30**

6853800	WHITE ROCK C NR BURR OAK, KS	Ref	588	0.16	0.09	**0.47**	**0.30**	**0.39**	**0.36**	0.24	0.23	**0.32**	**0.40**
6860000	SMOKY HILL R AT ELKADER, KS	Non-ref	9207	0.17	0.11	**0.26**	0.02	0.01	0.01	0.03	0.15	0.15	0.03
6861000	SMOKY HILL R NR ARNOLD, KS	Non-ref	13520	0.00	0.01	0.12	0.04	0.02	0.01	0.00	0.03	0.06	0.08
6866900	SALINE R NR WAKEENEY, KS	Non-ref	1803	**0.46**	**0.40**	**0.71**	**0.29**	**0.34**	**0.41**	**0.58**	**0.59**	**0.49**	**0.52**
6867000	SALINE R NR RUSSELL, KS	Non-ref	3890	**0.27**	0.20	**0.28**	0.17	0.18	0.23	**0.35**	**0.41**	**0.56**	**0.63**
6869950	MULBERRY C NR SALINA, KS	Ref	676	**0.32**	0.23	**0.44**	**0.49**	**0.46**	**0.44**	**0.37**	**0.34**	0.25	0.13
6872500	NF SOLOMON R AT PORTIS, KS	Non-ref	5996	0.12	0.12	**0.63**	0.15	0.18	0.20	0.11	0.19	**0.32**	**0.43**
6876700	SALT C NR ADA, KS	Ref	1052	**0.26**	0.10	**0.46**	0.24	**0.34**	**0.40**	**0.42**	**0.46**	**0.55**	**0.62**
6878000	CHAPMAN C NR CHAPMAN, KS	Ref	777	0.16	0.07	0.21	**0.27**	**0.27**	**0.26**	**0.27**	0.24	0.17	0.21

6882000	Big Blue River at Barneston, Nebr.	Non-ref	11518	0.07	**0.45**	**0.52**	**0.58**	**0.58**	**0.66**	**0.59**	**0.64**	**0.59**	**0.33**
6883000	Little Blue River near Deweese, Nebr.	Non-ref	2549	0.16	**0.26**	**0.43**	0.23	0.25	**0.30**	0.25	**0.28**	0.23	0.17
6884000	Little Blue River near Fairbury, Nebr.	Non-ref	6087	0.01	**0.44**	**0.32**	**0.43**	**0.46**	**0.53**	**0.41**	**0.49**	**0.42**	0.10
6885500	BLACK VERMILLION R NR FRANKFORT, KS	Ref	1062	0.22	**0.38**	**0.33**	**0.40**	**0.42**	**0.42**	**0.35**	**0.41**	**0.41**	0.22
6888500	MILL C NR PAXICO, KS	Ref	824	**0.54**	**0.60**	**0.54**	**0.53**	**0.57**	**0.60**	**0.59**	**0.65**	**0.64**	**0.30**
6889200	SOLDIER C NR DELIA, KS	Ref	386	**0.39**	**0.40**	**0.52**	**0.56**	**0.64**	**0.67**	**0.56**	**0.58**	**0.54**	**0.32**
6889500	SOLDIER C NR TOPEKA, KS	Ref	751	**0.51**	**0.39**	**0.44**	**0.44**	**0.48**	**0.49**	**0.42**	**0.45**	**0.48**	0.25
6892000	STRANGER C NR TONGANOXIE, KS	Ref	1052	**0.60**	**0.45**	**0.53**	**0.43**	**0.55**	**0.59**	**0.45**	**0.48**	**0.54**	**0.39**

6897500	Grand River near Gallatin, MO	Non-ref	5828	0.11	**0.39**	**0.52**	**0.44**	**0.50**	**0.59**	**0.52**	**0.52**	**0.41**	0.08
6903400	Chariton River near Chariton, IA	Ref	471	0.01	**0.53**	**0.80**	**0.52**	**0.67**	**0.72**	**0.75**	**0.70**	**0.54**	0.25
6906800	Lamine River near Otterville, MO	Ref	1406	0.40	**0.61**	**0.65**	**0.77**	**0.77**	**0.77**	**0.67**	**0.68**	**0.61**	0.19
6909500	Moniteau Creek near Fayette, MO	Ref	195	0.02	**0.43**	**0.41**	**0.40**	**0.49**	**0.64**	**0.67**	**0.57**	**0.31**	0.02
6910800	MARAIS DES CYGNES R NR READING, KS	Ref	458	**0.49**	**0.59**	**0.44**	**0.43**	**0.48**	**0.55**	**0.57**	**0.58**	**0.46**	0.11
6911490	SALT C AT LYNDON, KS	Ref	253	**0.36**	**0.54**	**0.39**	**0.34**	**0.43**	**0.55**	**0.62**	**0.60**	**0.45**	0.13
6917000	L OSAGE R AT FULTON, KS	Ref	813	**0.31**	**0.41**	**0.42**	**0.49**	**0.52**	**0.54**	**0.41**	**0.40**	0.22	0.11
6917060	Little Osage River at Horton, MO	Non-ref	1290	0.02	0.14	0.10	0.15	0.16	0.22	0.24	0.15	0.04	0.01
6918460	Turnback Creek above Greenfield, MO	Ref	653	0.16	**0.31**	**0.52**	**0.55**	**0.55**	**0.54**	**0.48**	**0.40**	0.23	0.02
6921200	Lindley Creek near Polk, MO	Ref	290	**0.36**	0.25	**0.28**	**0.54**	**0.50**	**0.45**	**0.30**	0.23	0.12	0.00

6923950	Niangua River at Tunnel Dam near Macks Creek, MO	Non-ref	1549	**0.26**	0.21	0.24	**0.36**	**0.39**	**0.44**	**0.39**	**0.28**	0.17	0.02
6926000	Osage River near Bagnell, MO	Non-ref	36260	0.17	**0.43**	**0.33**	**0.50**	**0.52**	**0.61**	**0.62**	**0.47**	**0.27**	0.01
6928000	Gasconade River near Hazelgreen, MO	Ref	3238	**0.33**	0.20	**0.31**	**0.57**	**0.57**	**0.53**	**0.36**	0.25	0.12	0.00
6928300	Roubidoux Creek above Fort Leonard Wood, MO	Ref	427	0.00	**0.28**	**0.46**	**0.47**	**0.54**	**0.56**	**0.49**	**0.51**	**0.31**	0.02
6930000	Big Piney River near Big Piney, MO	Ref	1450	0.01	0.10	0.25	**0.26**	**0.35**	**0.39**	**0.38**	**0.32**	0.19	0.02
7014500	Meramec River near Sullivan, MO	Ref	3820	0.00	**0.38**	**0.40**	**0.43**	**0.45**	**0.51**	**0.46**	**0.41**	**0.32**	0.17
7043500	Little River Ditch No. 1 near Morehouse, MO	Non-ref	1166	0.20	0.15	**0.52**	**0.37**	**0.47**	**0.49**	**0.47**	**0.39**	0.22	**0.29**

7057500	North Fork River near Tecumseh, MO	Ref	1453	**0.34**	0.09	**0.31**	**0.44**	**0.55**	**0.55**	**0.56**	**0.41**	**0.30**	0.19
7063000	Black River at Poplar Bluff, MO	Non-ref	3225	0.04	0.08	0.21	0.19	**0.29**	**0.38**	**0.62**	**0.57**	**0.28**	**0.34**
7066000	Jacks Fork at Eminence, MO	Ref	1031	0.00	0.24	**0.45**	**0.50**	**0.62**	**0.63**	**0.60**	**0.47**	**0.41**	0.22
7137000	FRONTIER DITCH NR COOLIDGE, KS	Non-ref	0	0.00	0.03	0.00	0.00	0.00	0.00	0.02	0.02	0.00	0.03
7137500	ARKANSAS R NR COOLIDGE, KS	Non-ref	65812	**0.61**	**0.72**	**0.87**	**0.45**	**0.52**	**0.59**	**0.68**	**0.65**	**0.72**	**0.81**
7138000	ARKANSAS R AT SYRACUSE, KS	Non-ref	66726	**0.51**	**0.71**	**0.83**	**0.40**	**0.48**	**0.55**	**0.66**	**0.59**	**0.64**	**0.83**
7142300	RATTLESNAKE C NR MACKSVILLE, KS	Ref	1805	0.22	0.18	0.23	0.06	0.11	0.18	0.22	0.25	**0.26**	0.14
7144780	NF NINNESCAH R AB CHENEY RE, KS	Ref	1847	**0.51**	**0.45**	**0.64**	**0.46**	**0.52**	**0.54**	**0.43**	**0.38**	**0.27**	**0.28**

7145700	SLATE C AT WELLINGTON, KS	Ref	399	**0.68**	**0.63**	**0.59**	**0.36**	**0.46**	**0.59**	**0.69**	**0.62**	**0.56**	**0.35**
7149000	MEDICINE LODGE R NR KIOWA, KS	Ref	2339	**0.56**	**0.52**	**0.49**	**0.31**	**0.36**	**0.48**	**0.54**	**0.52**	**0.60**	**0.35**
7157500	CROOKED C NR ENGLEWOOD, KS	Non-ref	2997	**0.59**	**0.44**	**0.46**	**0.46**	**0.52**	**0.56**	**0.58**	**0.52**	**0.53**	**0.29**
7167500	OTTER C AT CLIMAX, KS	Ref	334	0.23	**0.38**	**0.30**	0.21	**0.28**	**0.37**	**0.41**	**0.42**	**0.28**	0.07
7169500	FALL R AT FREDONIA, KS	Non-ref	2142	**0.35**	**0.62**	**0.55**	**0.48**	**0.57**	**0.70**	**0.70**	**0.67**	**0.50**	0.15
7184000	LIGHTNING C NR MCCUNE, KS	Ref	510	0.23	0.36	0.43	0.53	0.60	0.66	0.64	0.54	0.34	0.10